BRNO UNIVERSITY OF TECHNOLOGY

VYSOKÉ UČENÍ TECHNICKÉ V BRNĚ

FACULTY OF CHEMISTRY

FAKULTA CHEMICKÁ

INTITUTE OF MATERIAL SCIENCE

ÚSTAV CHEMIE MATERIÁLŮ

INVESTIGATION OF MORPHOLOGICAL CHANGES AND PROPERTIES OF SUPPORTED ZIEGLER-NATTA CATALYSTS DURING PROPENE POLYMERIZATION

STUDIUM MORFOLOGICKÝCH ZMĚN A VLASTNOSTÍ NOSIČOVÝCH ZIEGLEROVÝCH-NATTOVÝCH KATALYZÁTORŮ V PRŮBĚHU POLYMERACE PROPENU

SUMMARY OF PH.D. THESIS

TEZE DIZERTAČNÍ PRÁCE

AUTHOR AUTOR PRÁCE	**Ing. VÍT KOLOMAZNÍK**
SUPERVISOR ŠKOLITEL	**Dr. Ing. MIROSLAV SKOUMAL**

BRNO 2024

KEYWORDS

Polypropylene, Ziegler-Natta catalyst, prepolymerization, Stopped-flow, polymerization kinetics

KLÍČOVÁ SLOVA

Polypropylen, Zieglerův-Nattův katalyzátor, předpolymerace, Stopped-flow, polymerační kinetika

STORAGE PLACE

Brno University of Technology
Faculty of Chemistry,
Purkyňova 464/118,
CZ-612 00 Brno

MÍSTO ULOŽENÍ PRÁCE

Vysoké učení technické v Brně,
Fakulta chemická,
Purkyňova 464/118,
612 00 Brno

DECLARATION

I declare that my doctoral thesis was worked out independently and that the used references are quoted correctly and fully. The content of the above mentioned thesis is considered a property of BUT Faculty of Chemistry and can be used for commercial purposes only with the supervisor's and dean's consents.

……………………….
Student's signature

CONTENT

1 CURRICULUM VITAE 5
2 INTRODUCTION 7
3 THEORETICAL PART 8
  3.1 CATALYSTS FOR COORDINATION POLYMERIZATION 8
    3.1.1 Heterogeneous Ziegler-Natta Catalysts 8
    3.1.2 Mechanism of Polymerization of α-olefins on a Bimetallic Active Center 9
    3.1.3 Kinetics of Polymerization of α-olefins on Heterogeneous Ziegler-Natta Catalysts 10
  3.2 STOPPED-FLOW POLYMERIZATION 11
4 OUTLINE OF THESIS 12
5 EXPERIMENTAL PART 12
  5.1 CHEMICALS 13
  5.2 STRUCTURAL ANALYSIS METHOD 13
    5.2.1 SEC/GPC - Molar Mass Distribution Determination 13
    5.2.2 PSD - Particle Size Distribution 13
    5.2.3 MFR - Melt Flow Rate 13
    5.2.4 XS - Xylene Solubles 13
    5.2.5 ICP-OES - Ti Content 13
  5.3 4-LITRE BATCH REACTOR 14
    5.3.1 Procedure of 1st Method of the 1st Period 14
    5.3.2 Polymerization Data Processing 14
  5.4 3-PART CASCADE REACTOR 20
    5.4.1 Stopped-Flow Apparatus 21
6 RESULTS AND DISCUSSION 22
  6.1 1st POLYMERIZATION METHOD IN BATCH REACTOR 22
    6.1.1 Catalyst Activity upon Increasing the Temperature (1st Method of the 1st Period) 22
    6.1.2 The Impact of Temperature in the 1st Period of the 1st Method on Activity in the 2nd Period . 22
  6.2 3-PART CASCADE POLYMERIZATION 27
    6.2.1 Activation Zone of 3-Part Cascade Reactor 27
    6.2.2 Termination Zone of 3-Part Cascade Reactor 28
    6.2.3 Influence of Stopped-Flow 3-Part Reactor on Catalyst Performance 30
  6.3 CATALYST PREPOLYMERIZATION BY USING 3-PART CASCADE REACTOR 32
    6.3.1 PSD of Catalysts after 1st period of polymerization 32
    6.3.2 Effect of Prepolymerization in 3-Part Cascade Reactor 32

6.3.3 Influence of TEA/Ti Ratio on Activity and Kinetic Profile 33
7 CONCLUSION 34
8 REFERENCES 37

1 CURRICULUM VITAE

Name	Ing. Vít Kolomazník
Date of birth	14. 9. 1994
Email	Vit.Kolomaznik@vut.cz Kolomaznik.vit@seznam.cz
ORCID	https://orcid.org/0000-0003-1838-173X

Education and academic qualifications

2019– 2024 **Ph.D. program**
BUT, Faculty of chemistry, Chemistry of macromolecular materials

2017–2019 **Master's program (Ing.), pass with distinction**
BUT, Faculty of Chemistry, Chemistry, technology and properties of materials.

2014–2017 **Bachelor's program (Bc.)**
BUT, Faculty of Chemistry, Chemistry, technology and properties of materials.

Work experience

2024– present **Full-time chemical engineer in a chemical laboratory**
ORLEN Unipetrol RPA, s. r. o. – POLYMER INSTITUTE BRNO, o. z.
Tkalcovská 36/2, 602 00 Brno, Czech Republic

2019– 2024 **Part-time research assistant in a chemical laboratory**
ORLEN Unipetrol RPA, s. r. o. – POLYMER INSTITUTE BRNO, o. z.
Tkalcovská 36/2, 602 00 Brno, Czech Republic

Internships

2022 Student internship at the University of Alberta, Canada under the supervisor Professor João Soares, focused on mathematical optimization of kinetic profiles of α-olefin polymerizations

Publications

2023 Kolomazník V., Buráň Z., Skoumal M. *Effect of catalytic system on the structure of ethylene/propylene copolymers*, 11th International Conference on Chemical Technology, Brno, 2023, s. 150–155.
ISBN 978-80-88307-18-1

2023 Kolomazník, V., Cejpek, I. & Skoumal, M. *Temperature effect on the kinetic profile of Ziegler–Natta catalyst in propene polymerization*, poster in Blue Sky Conference on Catalytic Olefin Polymerization and the International

Conference on the Reaction Engineering of Polyolefins (INCOREP), Sorrento (Italy), 2023

2024	Kolomazník, V., Cejpek, I. & Skoumal, M. *Temperature effect on the kinetic profile of Ziegler–Natta catalyst in propene polymerization.* Chem. Pap. 78, 8397–8408 (2024). https://doi.org/10.1007/s11696-024-03679-w

Presentations at conferences

2023	Kolomazník, V., Cejpek, I. & Skoumal, M. *Temperature effect on the kinetic profile of Ziegler-Natta catalyst in propene polymerization*, Research presentation, Chemistry is Life, 2023, Brno University of Technology, Brno, awarded the Dean's Prize of the Faculty of Chemistry

Courses

2019	Advanced pedagogical study for teachers, completed by the final thesis and final exam, Brno, Continuing Education and Counselling Centre, Brno University of Technology

2 INTRODUCTION

The production of polymer materials was 1.7 million tonnes in 1950, 310 million tonnes in 2014 and is estimated to reach 1800 tonnes in 2050 [1]. For this reason, it is important to focus not only on the efficient use and recycling of polymers but also on the development of materials suitable for recycling. One of these polymers is polypropylene, widely utilized in many industries.

Karl Ziegler and Giulio Natta were crucial scientists in the global utilization of polyolefins. In October 1953, Karl Ziegler as a first person synthesised linear polyethylene using catalysts based on Cr, Zr, and Ti. Giulio Natta utilized Ziegler's results and successfully prepared isotactic polypropylene in March 1954 [2]. Since then, the development of Ziegler-Natta catalysts and methods of the ethylene and propene polymerization has undergone many changes and improvements. However, the exact polymerization mechanism isn't yet known. The most widely used model for the mechanism and kinetics description was proposed by Cossee in 1964.

Subsequently, other possibilities to prepare polyolefins with improved properties were discovered, such as the implementation of internal or external donors or prepolymerization. Over time, activity of the catalysts and isotactic part of polymers increased, while polydispersity (Đ) decreased. For better and more precise understanding of the mechanisms of α-olefin polymerization was developed stopped-flow technique, which can describe polymerization process in its early stages. Terano and Keii used SF for studying coordination catalysts for first time in 1987. The technique is able perform the polymerizations in very short times, on the order of hundredths and tenths of seconds. In such a short time, there is minimal influence of secondary polymerization reactions, such as monomer transfers or the formation of defects in the growing chain. Terano performed polymerizations with various reaction times and preparing polypropylene with very short molecular chains and a narrow distribution. Based on these results, he explained the kinetics polymerization in initiation phase. Furthermore, he clarified the process of particle growth, size, and distribution, confirming the theory of particle fragmentation.

Understanding the principles and mechanisms of polymerization is important not only at the scientific research level but also in the implementation of industrial production and the optimization of its processes. Only with a complete understanding of the fundamentals of polymerization reactions is it possible to predict the influences of used components, such as comonomers, electron donors, additives, or variable reaction conditions like polymerization temperature and pressure. All these knowledge leads to obtain materials with improved mechanical properties, reduce the energy of production and facilitate their easier recycling.

For this reason, the doctoral thesis deal with reaction conditions similar to industrial facilities. The utilized stopped-slow apparatus enables perform very short polymerizations and prepolymerizations at pressures and temperatures comparable to industrial reactors. The possibility of using these reaction conditions increases its application potential not only in academic research, but also for industrial purposes.

3 THEORETICAL PART

3.1 CATALYSTS FOR COORDINATION POLYMERIZATION

Discovery of Ziegler-Natta and Phillips catalysts in the early fifties caused the development of coordination catalysts for the polymerization of olefins. These were the first coordination catalysts used in coordination polymerization. Since that moment, these types of catalysts have undergone many improvements and changes. Both types of catalysts caused revolution in the field of polymer industry, and their potential allows for continuous enhancements even in present times. However, there was discovered another catalyst for coordination polymerizations. High efficiency metallocene catalysts were first used in the eighties and were complemented in the nineties by catalysts based on late transition metals [3]. The advantage of all these catalysts is ability creates of a monouniform microstructure with a broad molecular distribution. The reason is the presence of a greater number of active centers, which lead to the formation of chains with different properties, such as the molar mass of the producing chains, the amount of incorporated copolymer, stereoregularity, etc. In other words, the prepared polymer is a mixture of polymer chains formed at various active centers. There is no exact agreement regarding the number of active centers. Nevertheless, the distribution of molar mass and chemical composition deconvolution are commonly used today for their description. There is also no general agreement about their different behaviour, although several hypotheses have been proposed, such as differences in oxidation states or coordination with cocatalysts [3].

3.1.1 Heterogeneous Ziegler-Natta Catalysts

In general, heterogeneous Ziegler-Natta catalysts can be defined as a compound of a transition metal of the fourth to seventh groups, most often titanium or vanadium, and an alkylated metal of the first to third groups, known as a cocatalyst. The first ZN catalysts showed low activity and stereoregularity [4]. Despite heterogeneous ZN catalysts have undergone a long development, their modifications can be divided into four basic categories according to generation.

The low activity and the necessity to purify the catalyst residues were characteristic of first and second generation catalysts. These complications were one of the factors why a support for $TiCl_4$ was introduced in 1960 in third generation of ZN catalyst. The reason for support implementation was a very small amount of active $TiCl_4$, which was around 0.1 wt. % [5]. As a support was used magnesium chloride $MgCl_2$ in the form of spherical particles. Content of deposited titanium was around 1–3 wt.%.

The catalyst prepared with $MgCl_2$ support and activated with the cocatalyst (TEA) has an order of magnitude higher activity compared to previous generations, but the stereoregularity is very low. This problem was subsequently solved by the addition of a compound known as an electron donor [3, 6].

In the 1980s, the development of fourth-generation catalysts began with the discovery of the influence of combinations of external and internal donors. Ethyl benzoate was mainly used as internal donor and alkoxysilanes were used as external donors, especially diisobutyldimethoxysilane (DIBDMS), cyclohexylmethyldimethoxysilane (CHMDMS) or diisopropyldimethoxysilane (DIPDMS). Initially, when aromatic monoesters such as ethyl benzoate were used as an internal donors, the isotacticity increased from 40 to 60 wt. %. However, when aromatic monoesters, such as methyl p-toluate were also used as an external donors, the isotacticity of the polymer was around 95 wt. % (Table 1) [3].

Table 1: Overview of electron donors for Ziegler-Natta catalysts [3].

Internal donor	External donor	Isotacticity index [wt. %]
Aromatic monoesters (EB)	-	60
Aromatic monoesters (EB)	Aromatic monoesters (methyl p-toluate)	95
Aromatic diesters (DIBP)	Alkoxysilanes	97–99
Diethers (1,3-diether)	-	97–99

The regioselectivity and stereoselectivity of catalysts with diisobutyl phthalate (DIBP) internal donor depend on the alkoxysilane external donor [7]. In case of 1,3-diethers as internal donors, very high isotacticity (97–99 wt. %) can be achieved without external donors.

3.1.2 Mechanism of Polymerization of α-olefins on a Bimetallic Active Center

The first difference between monometallic and bimetallic mechanisms is in the reduction of $TiCl_4$ to a lower oxidation state by the cocatalyst. In the case of the bimetallic model, the organometallic cocatalyst is part of the active center and affects the polymerization mechanism (Figure 1) [8].

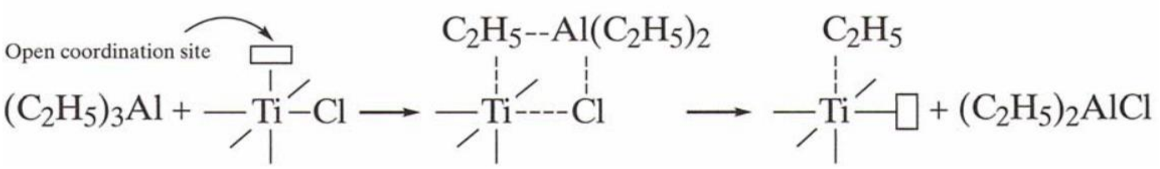

Figure 1: Formation of the ZN catalyst active center in the presence of a cocatalyst [2].

The cocatalyst alkyl group interacts with the vacancy orbital of the titanium catalyst, stabilizing the conformation of the transition state (Figure 2). After monomer insertion, the position of the vacant titanium orbital is restored at the same location of the active center [8].

Terano et al. predicted that the concentration of active centers decreases with the bulkiness of the alkyl group of the cocatalyst bound to titanium. The monomer interacts with the vacancy orbital of titanium to form a π-complex. Subsequently, maximal overlap of the bonding orbitals occurs. The orientation of the olefin molecule is determined by the polar interaction between its double bond and the C-Ti bond. The stereospecific orientation of the alkyl group depends on the steric interaction with the external groups on the aluminium atom. Subsequently, the insertion of the olefin with the π-complex into the Ti-C bond occurs according to Cossee's proposal, while the Al-C bond is broken. After insertion, the olefinic carbon C1 (according to IUPAC numbering) becomes the α-carbon of the polymer chain. The alkyl group CH2-CH(Et)-CH3 is bounded only to titanium and the C1 atom of the olefin molecule takes the place of the previous valence orbital. This rearrangement of atoms is preferred because of creating the coordination between the α-carbon of the polymer chain (C1 atom of the olefin) and the aluminium atom. In the end, active center is recovered, which is necessary to ensure stereoregularity [9].

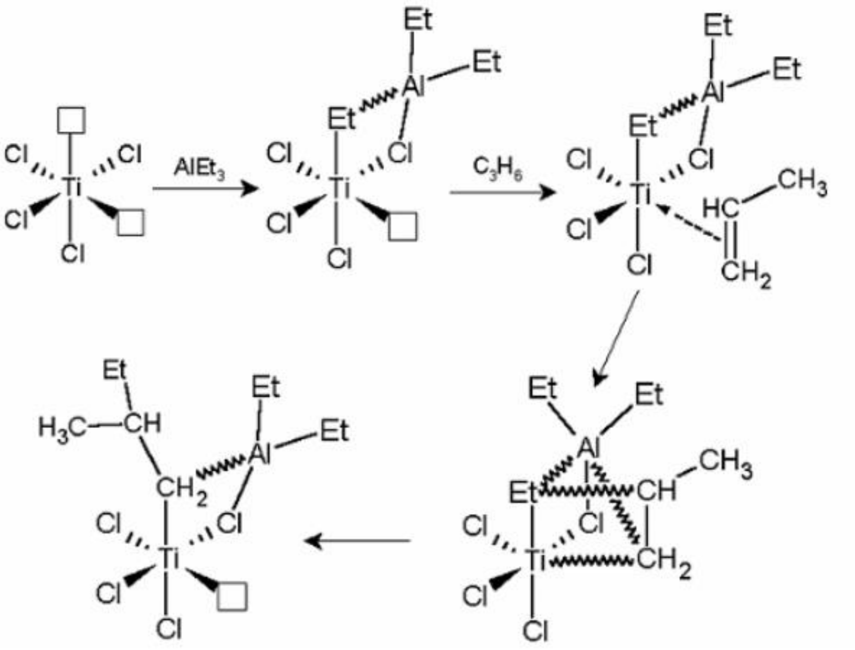

Figure 2: Polymerization mechanism on a Ziegler-Natta catalyst on a bimetallic active center [4].

3.1.3 Kinetics of Polymerization of α-olefins on Heterogeneous Ziegler-Natta Catalysts

The rate of polymerization on Ziegler-Natta catalysts is not constant. First of all, the formation of the active center occurs. Its formation occurs approximately 0.01 s after the start of the reaction, with the resulting active form being completed within the first tenth of a second [10].

The time dependence of the homopolymerization rate of ethylene and propene is shown in Figure 3. Comparison shows that the kinetic profiles of the polymerization of the two monomers are very different [11]. In the case of propene polymerization, the very sharp increase in the polymerization rate occurs almost immediately, followed by a gradual decrease. In the case of ethylene polymerization, the situation is different. The rate of polymerization slowly increases until it reaches a constant value and then the polymerization rate is stable for several hours.

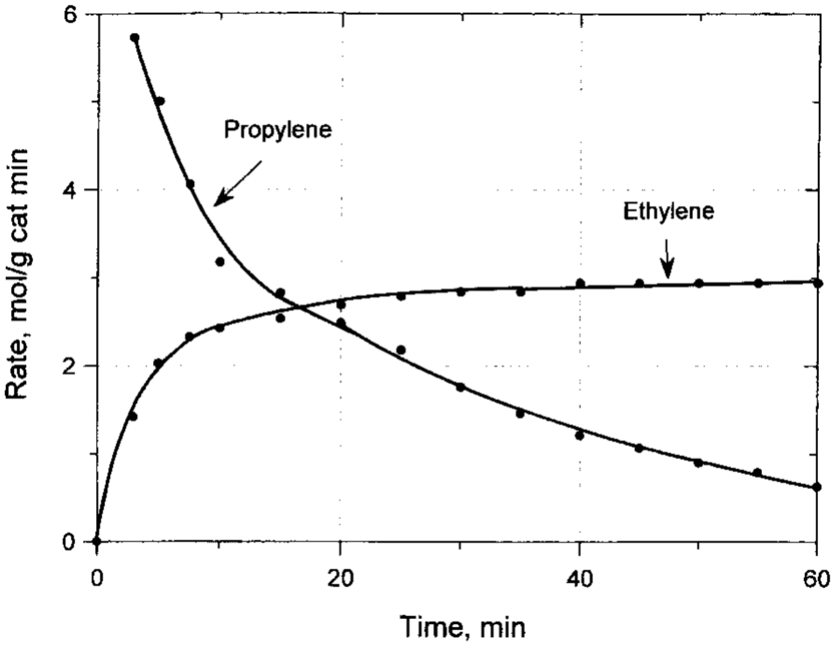

Figure 3: Comparison of homopolymerization kinetics of ethylene and propene on $TiCl_4$*/DIBP/*$MgCl_2$ *catalyst system with TEA/PhSi(OEt)*$_3$ *cocatalyst mixture* [12]*.*

3.2 STOPPED-FLOW POLYMERIZATION

long polymerization time (1–2 hours) in industrial polymerization causes transfers that lead to inhomogeneity of the system. In addition, the activity of the catalyst varies with the polymerization time [12]. The stopped-flow method was developed to study polymerizations with extremely short times (0.1–0.2 s) without these transfers. SF allows polymerization which is shorter than the lifetime of a growing chain (Figure 4) [13]. The stopped-flow method has been shown to be one of the most suitable techniques for studying the creation of active centers

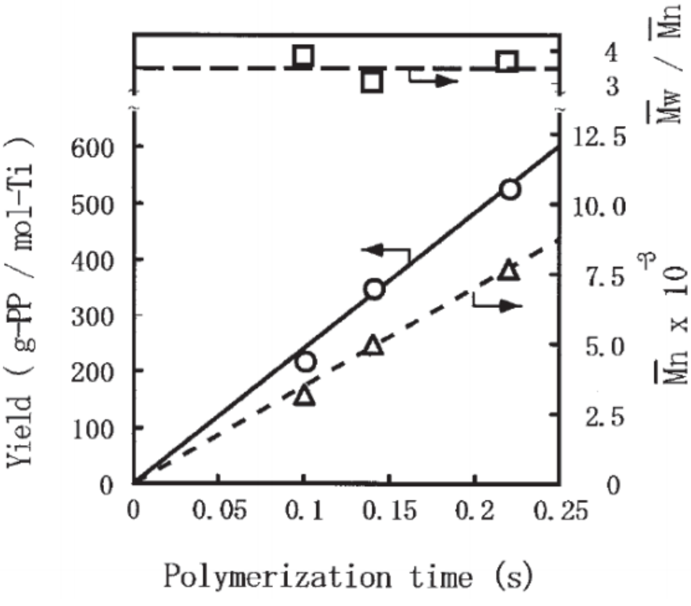

Figure 4: Dependence of yield, M_n *and polydispersity (*M_w/M_n*) on polymerization time in SF polymerization of propene using* $TiCl_4$*/ethyl benzoate/*$MgCl_2$ *based catalyst* [13]*.*

4 OUTLINE OF THESIS

The aim of the research is to study the influence of different polymerization methods of the 1st period on the kinetic profile of the 2nd main period of bulk polymerization and on the properties of produced polymer (Table 2). Kinetic profiles of polymerizations are described and evaluated by two models.

The thesis compares two different methods of the 1st polymerization period with conditions similar to the industrial process. As 1st method of the 1st period was chosen 10 min polymerization in batch reactor at different temperature levels in 350 ml of liquid propene. There were 7 temperature levels from 10 °C to 70 °C. In addition, at the temperature levels of 20 and 40 °C, the effect of the cocatalyst per titanium ratio was also described. For the 2nd method of the 1st period a stopped-flow apparatus was used. In this case, the catalyst was exposed to conditions similar to stopped-flow polymerization and prepolymerized in 3-part cascade reactor. The resulting SF prepolymerized catalyst was reversibly terminated with carbon dioxide and isolated. After isolation the SF prepolymerized catalyst was transferred to the mineral oil and utilized for propene polymerization in stainless steel batch reactor.

The 2nd period of polymerization was carried out at 70 °C for 90 min with 32 mmol of hydrogen. The kinetic profiles of the 2nd polymerization period are described by two different models based on fundamental functions according to the first and second order. The obtained kinetic constants of these models describe the behaviour of the prepolymerized catalyst during polymerization in liquid propene.

Table 2: Description of the individual phases of the polymerization process.

Polymerization process consisting of two periods		
	1st period	2nd period
a)	1st method – Batch prepolymerization in 4-litre reactor, 10 min, temp. levels 10–70 °C, 350 cm^3 of liquid propene	Batch polymerization in 4-litre reactor, 70 °C, 90 min, 1100 g of propene
b)	2nd method – SF prepolymerization in 3-part cascade reactor 40 °C, 2.1 MPa	

5 EXPERIMENTAL PART

For the polymerizations the 4-litre stainless steel reactor and the polymerization methods developed at ORLEN Unipetrol RPA, s. r. o. – POLYMER INSTITUTE BRNO, o. z. were utilized. In addition to the 4-litre stainless steel batch reactor, the stopped-flow apparatus was used for the 1st period of polymerization. Due to the need to isolate the prepolymerized catalyst without deactivation, the stopped-flow apparatus was modified and new method for catalyst capture and isolation was developed.

5.1 CHEMICALS

The polymerization grade propene was obtained from the PP plant (Orlen Unipetrol RPA, s. r. o., Litvinov, Czech Republic). The propene was further purified by passing through six purification columns.

Triethylaluminium cocatalyst with ultra-low aluminium hydride content (< 0.05 wt. %, TEA-ULH grade) originated from Lanxess (Germany) was used as n-heptane solution.

The commercial polymerization catalyst was obtained as a dry powder from an external company. The catalyst was transferred to the mineral oil (Shell Ondina Oil 933). The final catalyst concentration in the mineral oil slurry was about 25 wt. %.

5.2 STRUCTURAL ANALYSIS METHOD

5.2.1 SEC/GPC - Molar Mass Distribution Determination

The molar mass of polymers was determined by SEC/GPC analysis. The measurements were performed on a SEC/GPC Polymer Char instrument containing two columns. As the stationary phase was utilized a 7.8×300 mm PLgel Olexis with a 13 µm grain size..

5.2.2 PSD - Particle Size Distribution

The particle size distribution (PSD) is measured on a Mastersizer 2000 Malvern laser analyser, which is equipped with a dispersion unit (Hydro 2000MU) with a corresponding measuring cell. The measurements are carried out according to ISO 13320-1:2020 Particle size analysis - Laser diffraction methods.

5.2.3 MFR - Melt Flow Rate

The melt flow rate measurement is based on ISO 1133-1:2022 on a MI-ROBO instrument from GÖTTFERT. The sample was stabilized with 0.5 wt. % BHT. Measurement was performed at 230 °C with a mass load 2.16 kg.

5.2.4 XS - Xylene Solubles

The measurement of xylene soluble fraction of polypropylene is based on the standard method ISO 16152:2022(E) "Plastics - Determination of the xylene soluble fraction in polypropylene". 0.5 g of polymer sample was dissolved for 1 h in 25 ml of o-xylene at 135 °C. Precipitate of crystalline fraction is filtered and polymer content remaining in solution (XS) is evaluated using FIPA instrument with GPC column (Malvern Instruments Ltd).

5.2.5 ICP-OES - Ti Content

Spectro Blue instrument from SPECTRO CS was used for the ICP determination of Ti in prepolymerized catalyst. Measurements with detection limit 0.02 mg/l were evaluated by Smart Analyzer Vision Software Version 6.01.0951.

5.3 4-LITRE BATCH REACTOR

5.3.1 Procedure of 1st Method of the 1st Period

The defined amount of TEA diluted by n-heptane was charged to the reactor by micropipette Microman (Gilson). Then the reactor was filled with defined amount of propene leading to the constant liquid phase volume 350 ml at various prepolymerization temperatures. Concurrently with propene 32 mmol of hydrogen was added. After stabilization of the starting polymerization temperature, the catalyst suspension was charged by Microman micropipette into the catalyst injection device. Subsequently, the catalyst was injected to the reactor by a flush of 40 g of liquid propene. In all experiments the final volume of liquid propene during the 1st polymerization period of 1st method remained constant at 350 ml.

5.3.1.1 Short Isothermal Experiment

After the catalyst injecting the polymerization proceeded at constant temperature and stirring speed 630 rpm for 10 min. Afterwards, the reactor was vented and the mass of the polymer was determined.

5.3.1.2 Sequential Two Periods Experiment

After the catalyst injection, the 1st method of the 1st polymerization period at defined temperature level was carried out for 10 min. The reactor was then filled with a further dose of propene to total amount 1100 g followed with temperature raise to 70 °C. In the case of the 2nd method of the 1st polymerization period (described in Chapter 5.4), the filling of the reactor with propylene up to 1100 g is carried out first. The 2nd polymerization period was started after reaching 98 % of the main polymerization temperature (i.e. 68.6 °C of 70 °C). The 2nd polymerization period was carried out at 70 °C in liquid propene for 90 min. During the whole 2nd polymerization period additional propene flow of 250 g/h was applied to the reactor to approximately compensate the consumed propene.

5.3.2 Polymerization Data Processing

5.3.2.1 Data Collection

The Figure 5 shows that during the experiment the liquid propylene temperature was monitored using the thermocouple Tr located at the bottom of the reactor, and the temperature of the gas phase using the thermocouple Tr2 placed close to the reactor cover. The temperature of the incoming water reactor jacket was monitored by the thermocouple Tw. During the polymerization, the special double-ribbon stirrer with bottom blades was rotated at 630 rpm to ensure temperature homogeneity throughout the reactor, and all internal walls were in contact with the liquid propene. This statement was supported by the same readings from both internal thermocouples, Tr and Tr2. With such conditions, the technical arrangement of the 4-litre reactor allowed the heat flow released by the polymerization reaction to be monitored.

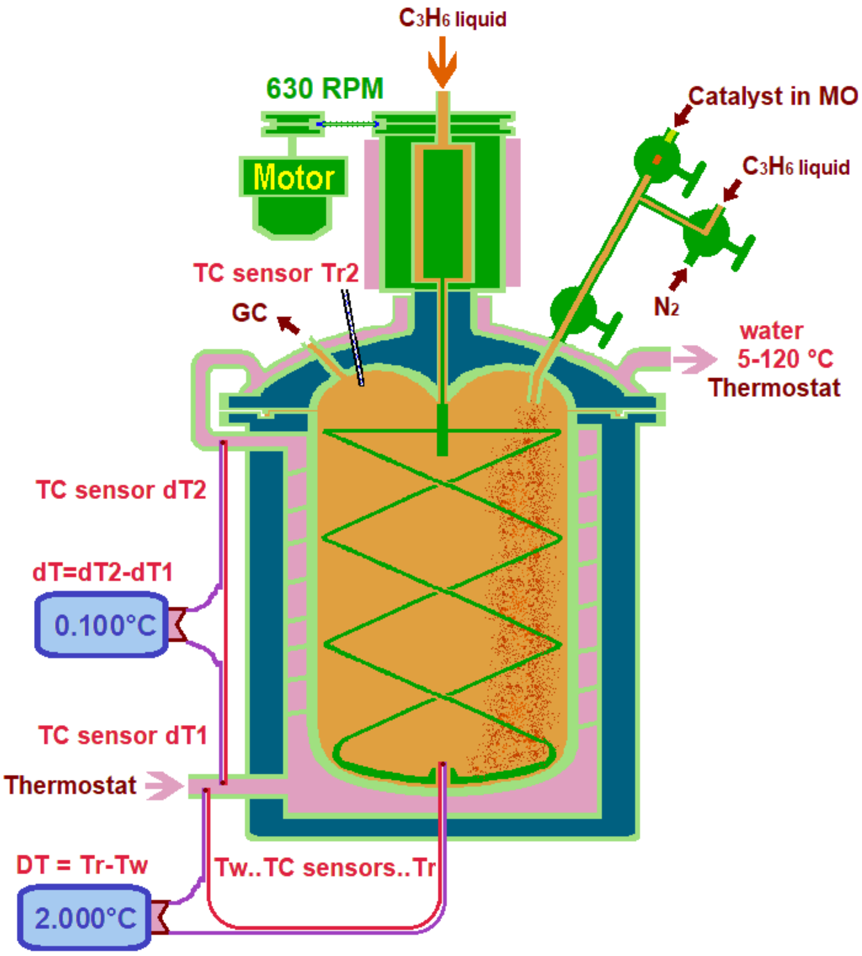

Figure 5: Scheme of 4-litre reactor for propene polymerization in liquid phase.

5.3.2.2 Polymerization Data Evaluation

The heat signal was automatically corrected for temperature scatter using a calibrated linear function of instant temperature and its derivation. All the collected DT (Tr-Tw, $\Delta T \approx 2.0$ °C) points are depicted in light blue "DT(all)", while the dark blue points "DT(incl)" correspond to those used for kinetic curve fitting. Example collected data are depicted in Figure 6.

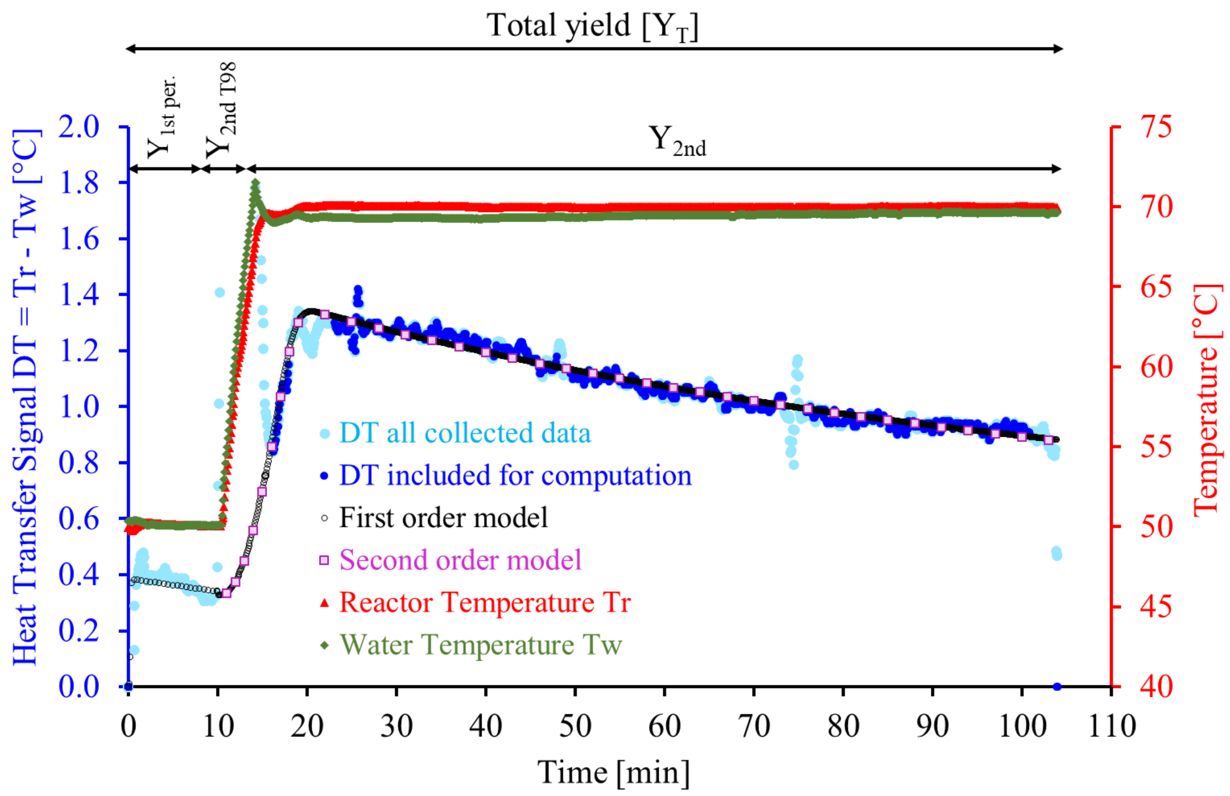

Figure 6: Example of 2-step polymerization data record with 1^{st} method of 1^{st} period. Polymerization started at 50 °C, after 10 min the temperature it was gradually increased to 70 °C; $T_{1st\ per.}$: Temperature in the 1^{st} polymerization period; $Y_{1st\ per.}$: Polymer yield in the 1^{st} period; $\mathrm{Y}_{2nd\ T98}$: Polymer yield between end of 1^{st} period and temperature rise to T_{pol} = 98 % (=68.6 °C); Y_{2nd}: Polymer yield between temperature rise to T_{pol} = 98 % and end of 2^{nd} polymerization period; Y_T: Total yield.

5.3.2.3 Kinetic Function

The polymerization process starts immediately after the activated catalyst comes into contact with propene. This sub-second starting phenomenon is not detectable by the reactor as set up, even if the catalyst is charged at the final 70 °C temperature level, because the charging procedure disturbs the temperature reading for about 1–2 min. On the other hand, if the catalyst is charged at a lower temperature than the final polymerization level, significant activity increase is observed even several minutes after the final polymerization temperature is reached. Thus, the acceleration patterns of the polymerization kinetics are governed not only by the increasing temperature between the periods, but also by the time itself. To include this observation in the polymerization kinetic computation for the whole polymerization period, suitable compensation for the activity increase has to be included in the kinetic functions. To facilitate the subsequent kinetic profile computation deceleration, a simple mathematic approach was chosen to describe the catalyst activity increase between the polymerization periods, based on the linear combination of two non-dimensional transition functions separately describing the temperature increase and also the final polymerization rate increase after the final temperature is reached:

$$\mathrm{Acc}(t) = \frac{1}{2}\cdot\left\{1-e^{\left[-\left(\frac{t}{K_{a1}}\right)^{P_1}\right]}+1-e^{\left[-\left(\frac{t}{K_{a2}}\right)^{P_2}\right]}\right\} \qquad (1)$$

Where t is time since the catalyst injection into reactor (i.e. activation), K_{a1}, K_{a2}, P_1 and P_2 are the process activation parameters.

The function (1) applied in combination with deceleration functions facilitates the transition of the polymerization rate level from zero at zero time to an increased level after which Acc(t) = 1. However, this research is focused namely on the 2nd polymerization period, and zero time is defined as the end of the 1st polymerization period, when catalyst activity is already significant. Thus, additional modification of the acceleration function (1) is necessary:

$$\mathrm{Acc}(t) = A_{1i} + \frac{1}{2}\cdot\left\{1-e^{\left[-\left(\frac{t}{K_{a1}}\right)^{P_1}\right]}+1-e^{\left[-\left(\frac{t}{K_{a2}}\right)^{P_2}\right]}\right\} \qquad (2)$$

Where t is the time since the end of the first polymerization period, A_{1i} is a constant dimensionless parameter that allows us to compute the polymerization rate profile of the 2nd polymerization period from the final polymerization rate reached at the end of the 1st polymerization period.

The infinity time limit of the acceleration function (2) is defined as:

$$\mathrm{Acc}(\infty) = A_{1i} + 1 \qquad (3)$$

During the process of polymerization kinetic parameters optimization the parameter A_{1i} is constant. Its value is derived from the experimentally assessed yield of short 10 min runs performed in the same way as the 1st polymerization period of the sequential runs.

At the beginning of the temperature increase between the 1st and 2nd periods, the experimental DT points are not applicable as input data for optimization of the process activation parameters of the acceleration function due to their large scatter caused by the high power of the thermostat heaters enabling the fast temperature increase. Thus, at the beginning of the temperature increase, the parameters are optimized according to the instant temperature reading and in the context of the experimentally verified dependence of catalyst activity on the instant temperature (Figure 7). Before 70 °C is reached, the thermostat heaters are automatically switched to a mode in which they maintain the polymerization temperature level. Then, the kinetic profile can be evaluated directly using experimental DT points automatically corrected for the instant reactor temperature and its derivation.

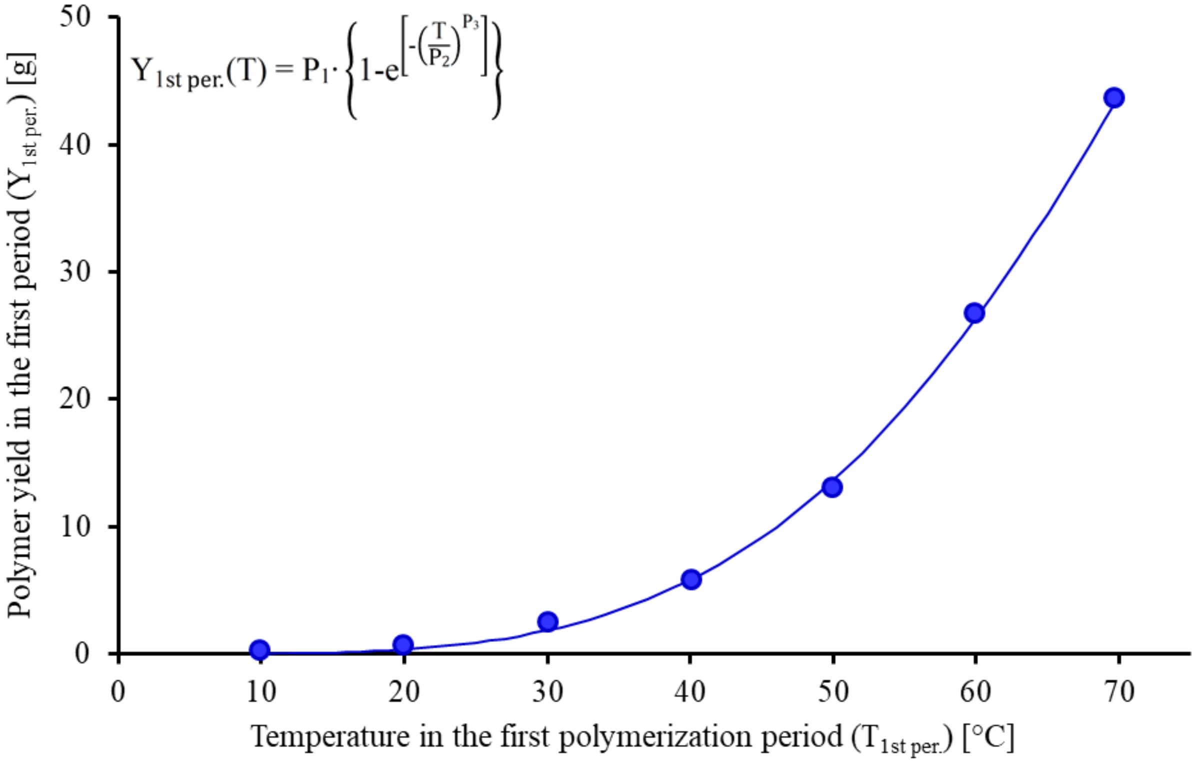

Figure 7: Effect of the temperature on polymer yield in the 1^{st} *period,* $T_{1st\ per.} = 10\text{–}70$ *°C, Volume of liquid propene = 350* dm^3 *of liquid propene;* $m_{cat.} = 4$ *mg, TEA/Ti = 120 mol/mol,* $n_{H2} = 32$ *mmol; t = 10 min*

After the highest polymerization activity, decrease in catalyst activity was observed. Two approaches were studied to describe the polymerization rate decrease:

1: Two types of polymerization active centers deactivation according to the first order:

$$\mathrm{Dec1^{st}(t) = A_{1f} \cdot e^{(-K_{d1f} \cdot t)} + A_{2f} \cdot e^{(-K_{d2f} \cdot t)}} \tag{4}$$

2: One type of polymerization active center deactivation according to the second order:

$$\mathrm{Dec2^{nd}(t) = \frac{A_{1s}}{1+K_{d1s} \cdot t}} \tag{5}$$

Where t is time since the end of the 1^{st} polymerization period, A_{1f}, A_{2f}, A_{1s} and A_{2s} are parameters corresponding to the polymerization rate at zero time of the deceleration functions, from which the active centers deactivate according to their deceleration nature described by the parameters K_{d1f}, K_{d2f} and K_{d1s}.

The zero time in our kinetic description is the end of the 1^{st} polymerization period, when the polymerization process proceeds at various temperature levels rendering to the process various polymerization rates. Thus, to fit the experimental DT points on the kinetic equation FDT over the entire 2^{nd} polymerization period, the simple product of the combination of deceleration functions (4) or (5) and the equation (2) was used:

$$\mathrm{FDT1^{st}(t) = Acc(t) \cdot Dec1^{st}(t)} \tag{6}$$

and

$$\mathrm{FDT2^{nd}(t) = Acc(t) \cdot Dec2^{nd}(t)} \qquad (7)$$

The experimental DT points profile (Figure 6) are assumed to be a linear measure of the instant polymerization rate, linearly transferable from their dimension (°C) to the dimension of the polymerization rate – $\mathrm{kg_{PP}/(g_{cat} \cdot h)}$:

$$\mathrm{Rp(t) = DTc \cdot FDT(t)} \qquad (8)$$

Where Rp(t) is polymerization rate profile; DTc is semi-empirical constant of the polymerization run; FDT(t) is profile fitted to experimental DT data according to equations (6) or (7).

The product of the acceleration and deceleration function defined using the equation (6) or (7) can easily describe polymerization start-up upon constant or increasing temperature. Another advantage of this practical approach is in the easy definition of the kinetic maximum of the polymerization rate Rp(0) at zero time of deceleration (theoretical instant acceleration, where K_{a1} and K_{a2} are zero), which results in the same equation as the extrapolation of the acceleration time to infinity – see the equations (1) and (2). Thus, the extrapolated kinetic maximum of polymerization rate according to the two kinetic approaches is defined as:

The 1st order of deceleration:

$$\mathrm{Rp1^{st}(0) = (A_{1i}+1) \cdot (A_{1f}+A_{2f}) \cdot DTc} \qquad (9)$$

The 2nd order of deceleration:

$$\mathrm{Rp2^{nd}(0) = (A_{1i}+1) \cdot A_{1s} \cdot DTc} \qquad (10)$$

Fitting the selected experimental points (dark blue) since the end of prepolymerization to the function (4) and (5) is depicted in Figure 6. The fitting procedure computes in several steps all parameters of the function (6) and (7), performing the best fit to the experimental DT points.

Computation of DTc is the next following step after fitting the DT points. According to the equation (8), each data point DT can be transferred into instant heat flow produced by the polymerization rate. Thus, the time integral of the fitted function FDT(t) (6) including the temperature start-up period, represents the total heat produced by the polymerization process, which corresponds to the total yield of polymer produced during the 2nd period, including the temperature-increase part of the 2nd period. Then, the multiplication factor DTc in the equation (8) valid for the second polymerization period can be computed as a simple ratio of the total yield (corrected for the amount of polymer developed during the 1st period) and the total heat computed as the integral FDT(t) from the end of the 1st period to the end of the 2nd polymerization period:

$$\mathrm{DTc} = \frac{\mathrm{Y_T\text{-}Y_{1st\ per.}}}{\int_{t1}^{t2} \mathrm{FDT(t)}dt} \qquad (11)$$

Where Y_T is the total polymer yield (1st + 2nd periods), as determined by the polymer weighting, Y_{1st} is the polymer yield produced in the first 10 min period calculated from the equation (12) and cumulative integral value of FDT(t) function (6).

$$Y_{1st\ per.}(T) = P_1 \cdot \left\{ 1 - e^{\left[-\left(\frac{T}{P_2} \right)^{P_3} \right]} \right\} \tag{12}$$

Where T is polymerization temperature, P_1, P_2 and P_3 are optimized parameters.

5.4 3-PART CASCADE REACTOR

The 2nd method of catalyst prepolymerization was carried out in stopped-flow apparatus. In this study, the classical stopped-flow capillary reactor was replaced by a 3-part cascade polymerization reactor (Figure 8) located in a 100-litre pressure vessel.

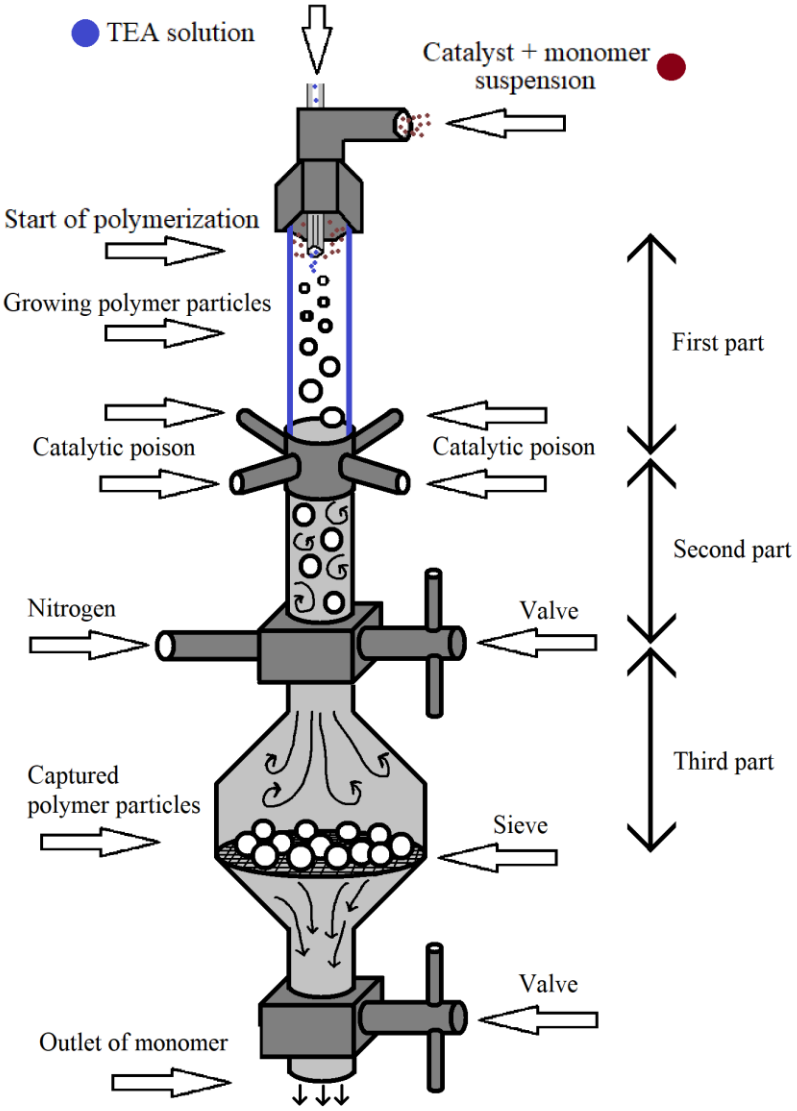

Figure 8: Scheme of 3-part cascade stopped flow reactor.

5.4.1 Stopped-Flow Apparatus

The high pressure stopped-flow facility was constructed at ORLEN Unipetrol, s. r. o. – POLYMER INSTITUTE BRNO, o. z. by Hoza and Cejpek. Hoza used it for research on P/E copolymers [14] and by Tvrdý it was utilized for the kinetic study [86]. Its design enables polymerization in a very short time scale and under the conditions close to an industrial production process.

The Stopped Flow apparatus consists of the following main parts (Figure 9):

- A 6-litre water-tempered stainless steel pressure vessel (green), which was used as a storage vessel for the catalyst suspension in liquid propene. It was filled with 2500 g of propene before the start of each experiment.
- An 8-litre water-tempered stainless steel pressure vessel (purple) used as a storage vessel for the terminating agent in liquid propene.
- A special device for dosing the TEA solution in n-hexane based on a piston flow of the TEA solution in a 12 m long stainless steel pipe with an internal diameter of 4 mm (blue container).
- 100-litre stainless steel pressure vessel (max. pressure 2.2 MPa) with 3-part cascade reactor inside. The absence of mixing allows the pressure in the vessel to be kept constant, regardless of the temperature of the components located inside the vessel.

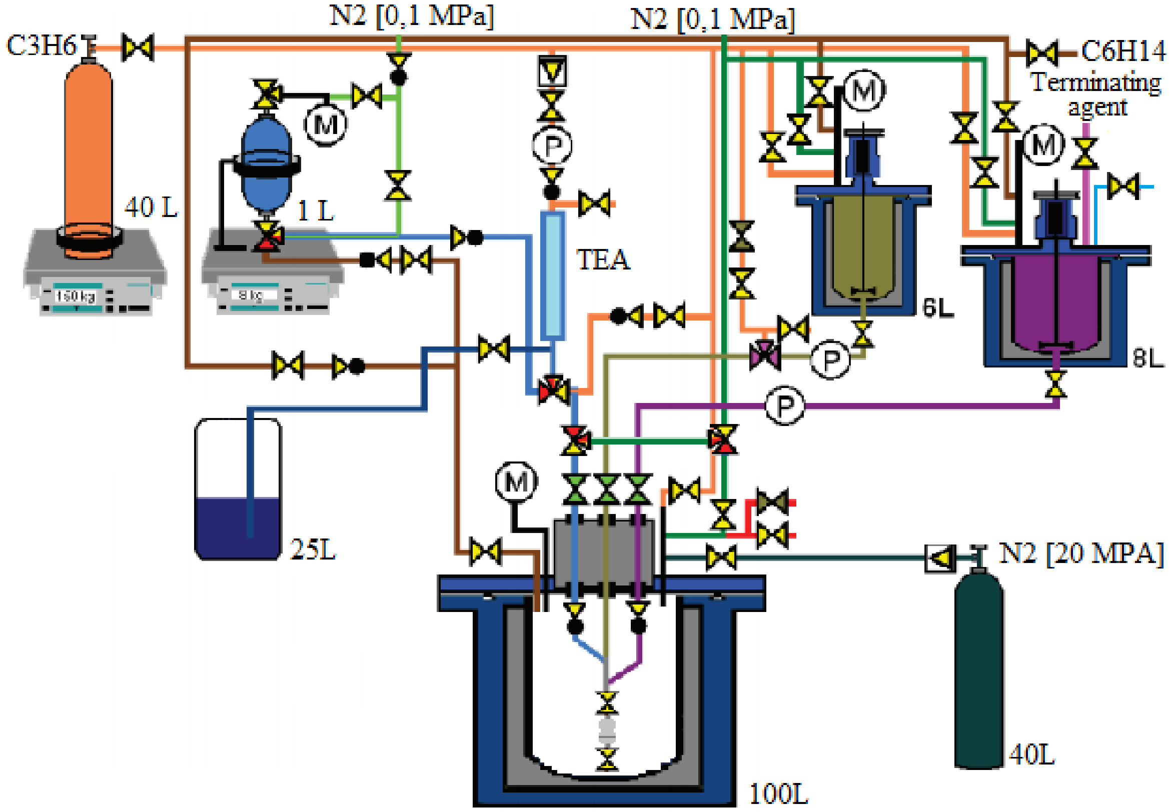

Figure 9: Scheme of stopped-flow polymerization apparatus [14].

6 RESULTS AND DISCUSSION

6.1 1st POLYMERIZATION METHOD IN BATCH REACTOR

6.1.1 Catalyst Activity upon Increasing the Temperature (1st Method of the 1st Period)

Within the scope of this two-polymerization-period research, we separately investigated the effect of different temperatures in the range 10–70 °C on catalyst activity during the 1st period in the short isothermal experiment mode (Chapter 5.3.1.1).

The results of this set of runs are depicted in Figure 7. The experimental polymer yield points corresponding to the temperature levels are fitted by a function constructed according to the transition function (1) described above in the context of the kinetics acceleration in equation (12).

A plausible explanation for the described increase in polymerization activity with a decrease in polymerization temperature during the catalyst activation period is related to the monomer-dimer equilibrium of TEA. At a lower temperatures, TEA occurs in dimer form which is unable to create an active center on the catalyst. Thus, after the catalyst is introduced into the reactor at low temperature, the formation of the active center upon dissociation the TEA dimer occurs slowly during the temperature ramp between the polymerization periods, and the polymerization heat is easily transferred into the surrounding space of the catalyst particles.

6.1.2 The Impact of Temperature in the 1st Period of the 1st Method on Activity in the 2nd Period

This study was focused on the catalyst performance using the results of 10 min isothermal polymerizations described in Chapter 6.1.1 and the subsequent widening of the scope by searching the catalyst performance during the 90 min after the reactor was heated to 70 °C. Naturally, the duration of the temperature increase depends on the temperature difference between the 1st and 2nd polymerization periods. To facilitate the definition of the end of the temperature increase phase, the limit of 98 % of the targeted 70 °C level (68.6 °C) was defined as the important milestone, after which the duration of the 2nd period was counted until the next 90 min time elapsed.

As the temperature levels in the 1st period were the only variable in this study, all the resulting values in the relevant comparisons for all 14 runs performed at seven temperature levels (two runs at each level) were related to the temperature levels. At first, polymer yields between the milestones of the entire process are shown in Figure 10.

The data related to polymer yield formed in the 1st period were already discussed above in Chapter 6.1.1. The yields were directly determined by weighting the polymer yield obtained from the reference 10 min experiments. Similarly, the total polymer yield obtained after the whole experiment (1st + 2nd periods) was also determined by simple weighting.

On the other hand, the most important value – the polymer yield formed during 90 min at a constant temperature of 70 °C is inherently connected with polymer yield formed during the intermediate temperature increase that lasted over various periods ($Y_{2nd\ T98}$). The most suitable solution to the intermediate yield evaluation is based on computing the overall polymerization kinetics describing the whole 2nd period, including the temperature increase.

Then, the intermediate yield during the temperature increase phase ($Y_{2nd\ T98}$) is evaluated as the integral of the kinetic function until the defined limit of 98 % of the targeted 70 °C level (i.e. 68.6 °C) is reached. The functional construction for the description of the polymerization rate acceleration during the intermediate period defined by the equation (1) was already found to be in congruence with the experimentally constructed polymerization yield dependence on the temperature in the equation (12). Also, further indirect support of the correctness of this approach is the independence of DTc (11) on the temperature differences and also on the duration of the intermediate period. This independence is demonstrated in Figure 10.

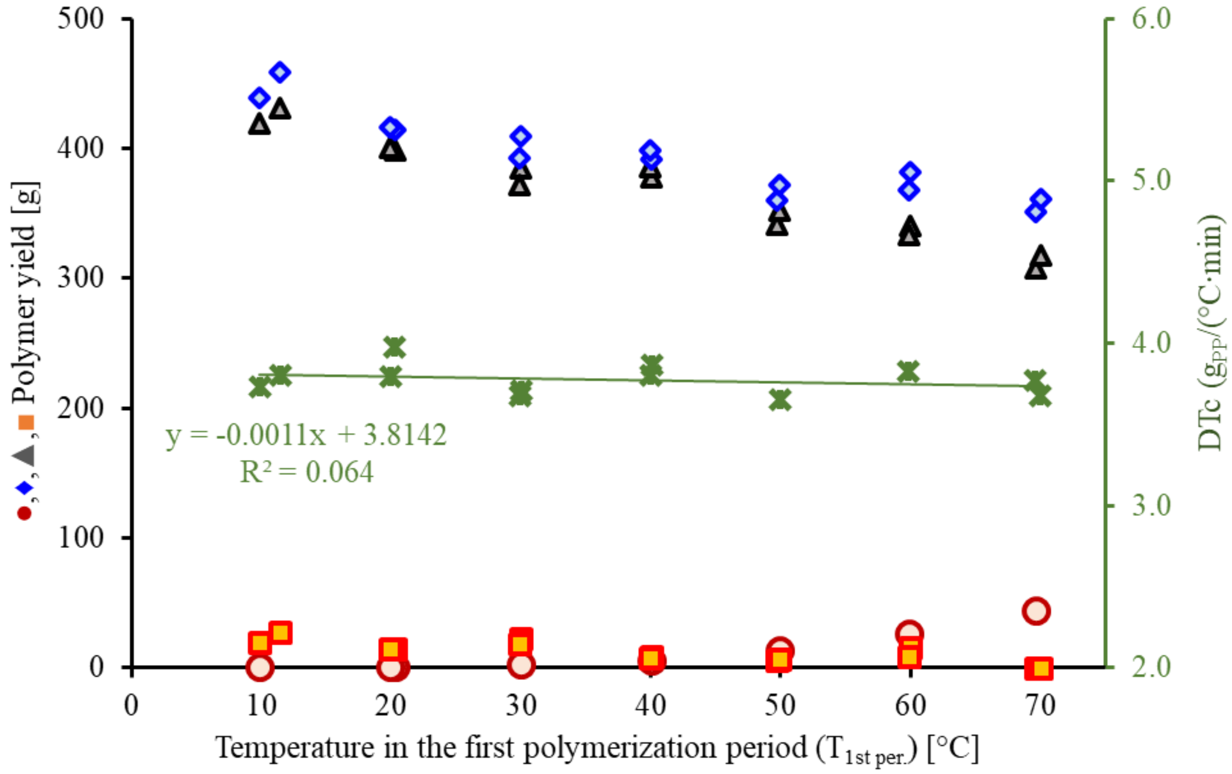

Figure 10: Polymer yield in 1st and 2nd polymerization periods, m_{cat} *= 4 mg, TEA/Ti = 120 mol/mol,* n_{H2} *= 32 mmol;* ○ $Y_{1st\ per.}$ *(10 min at various temperatures);* □Y_{2ndT98} *(The yield produced during the temperature rise from the end of 1st period to 68.6 °C);* ▲ Y_{2nd} *(90 min after the temperature reached 68.6 °C);* ♦ Y_T *(whole yield of sequential run);* × *DTconst (DT constant of the polymerization run).*

Computation of the polymerization kinetics as described in the Chapter 5.3.2.3 was performed automatically for both kinetic approaches in relation to the active center aging process, the equations (4) and (5). Computing all 14 runs of this experimental series revealed that the resulting optimized K_{d2f} values are close to zero, which indicate not realistic statement about their everlasting performance. In other words, it was revealed that the aging of the more stable active centers according to the first order of their decay is negligible. Thus, the equation (4) could be modified as follows:

$$\mathrm{Dec1}^{st}(t) = A_{1f}\cdot e^{(-K_{d1f}\cdot t)}+A_{2f} \tag{13}$$

Then, the kinetic computation of all results of the 14 runs was repeated for the equations (7) and (13). A typical example of the comparison of the best fit to the experimental points for both kinetic approaches is exemplified in Figure 6.

The resulting comparison of the kinetic profiles of the seven temperature levels for the first order approach and single selected runs from the duplicates is depicted in Figure 11 and, for the second order, in Figure 12.

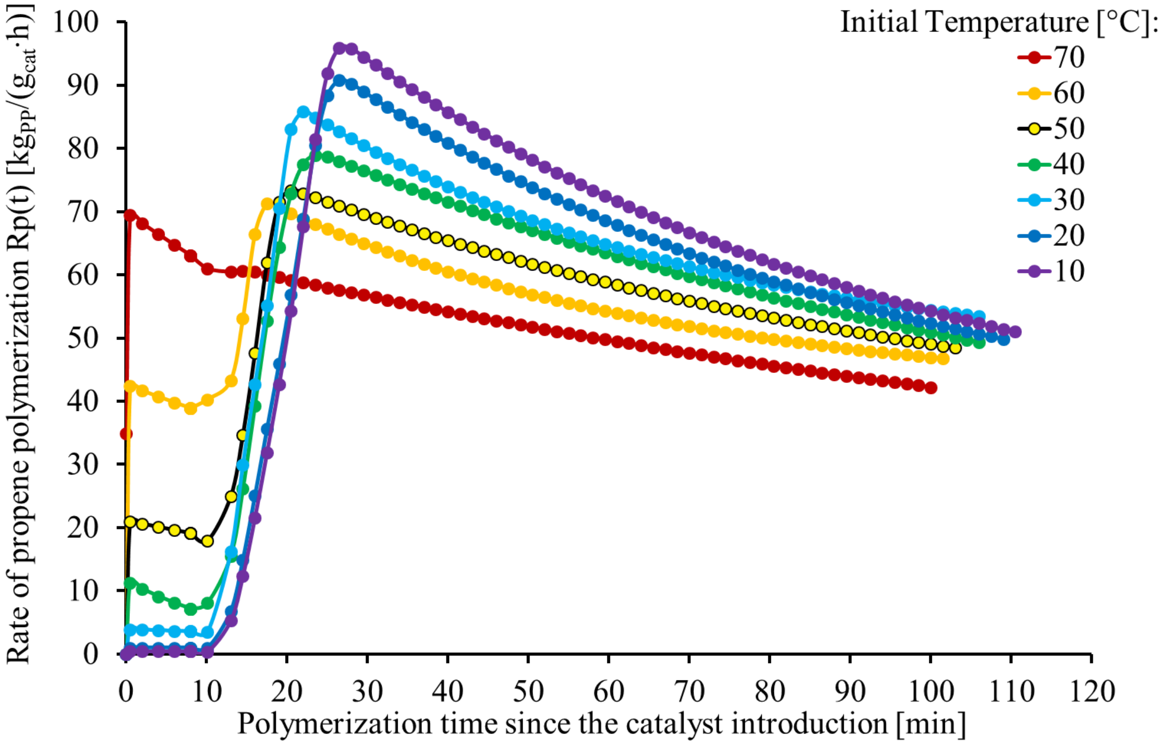

Figure 11: Polymerization kinetic profiles assuming the first order of deceleration; m_{cat} *= 4 mg, TEA/Ti = 120 mol/mol,* n_{H2} *= 32 mmol.*

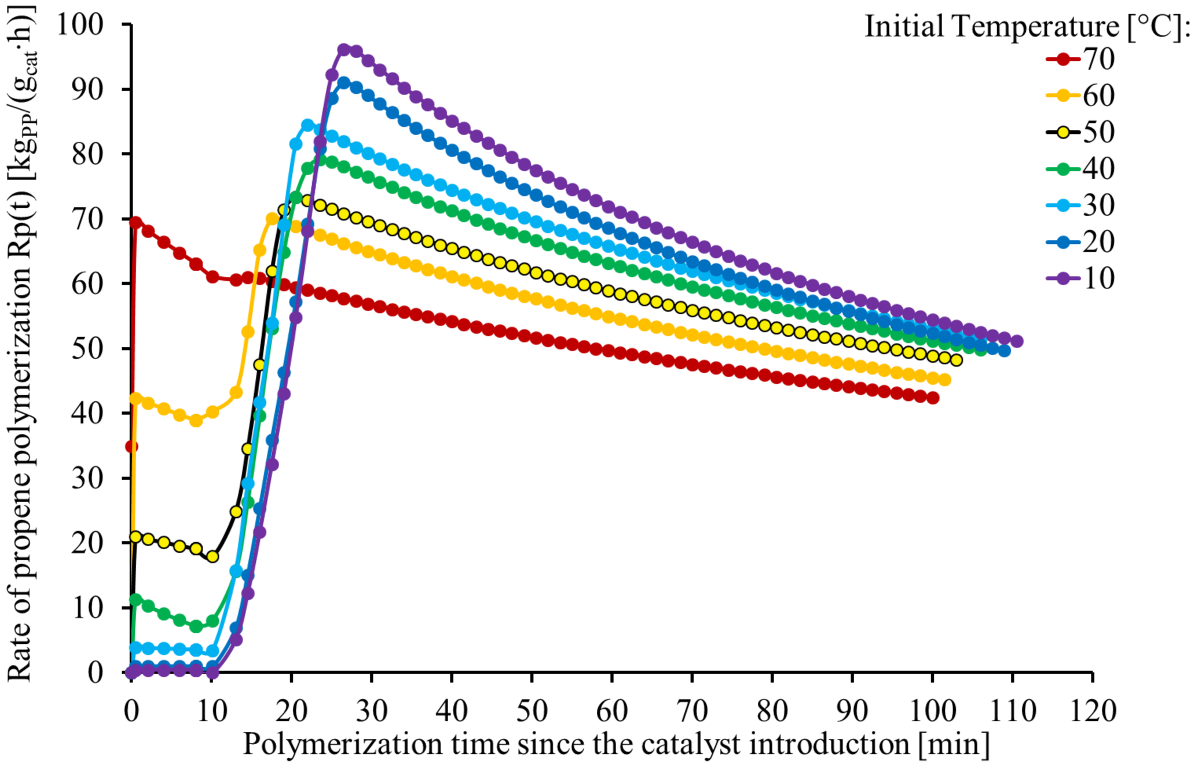

Figure 12: Polymerization kinetic profiles assuming the second order of deceleration; m_{cat} *= 4 mg, TEA/Ti = 120 mol/mol,* n_{H2} *= 32 mmol.*

The almost identical kinetics of the relevant profiles are shown in Figure 11 and Figure 12. Although the shape of the curves was calculated in the same manner as described above for the 2nd period, their accuracy is limited due to the relatively small volume of the liquid phase inside the reactor. This situation could be a source of error in the interpretation of the heat transfer data because the smaller volume may not fully cover the entire inner surface of the reactor. However, the instant activity at the joint point for both periods (10 min) is assessed with high accuracy, because it corresponds to the average activity calculated from the experimental yields of the short (10 min) isothermal runs discussed in Chapter 6.1.1 and presented in Figure 7.

After 10 min the kinetic curves in Figure 11 and Figure 12 enter into the polymerization temperature increase stage, which corresponds to their sharp increase to maximum polymerization rate, typically occurring during several minutes after the temperature level of 70 °C is reached (Figure 6).

Optimized parameters for both kinetic approaches might also be in good correlation with the only variable in this research – the polymerization temperature in the 1st period (Figure 13 and Figure 14).

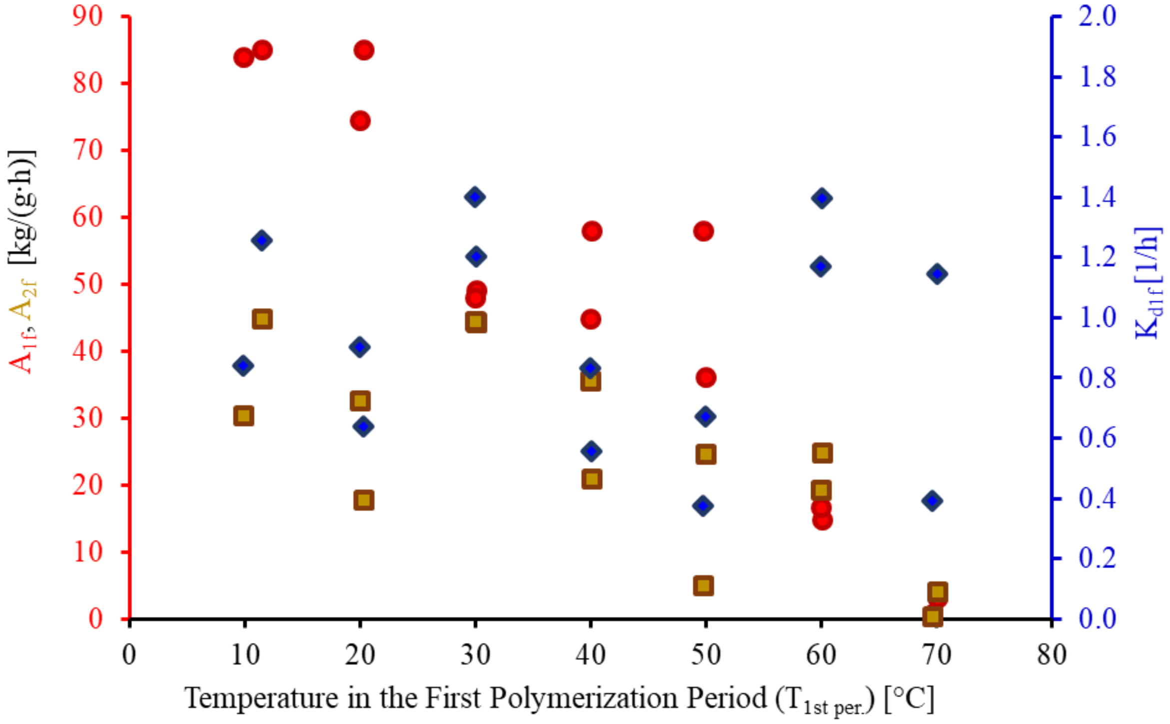

Figure 13: Comparison of optimized parameters for the first order of deceleration, ●A_{1f}, ■A_{2f}, ♦K_{d1f}; m_{cat} = 4 mg, TEA/Ti = 120 mol/mol, n_{H2} = 32 mmol.

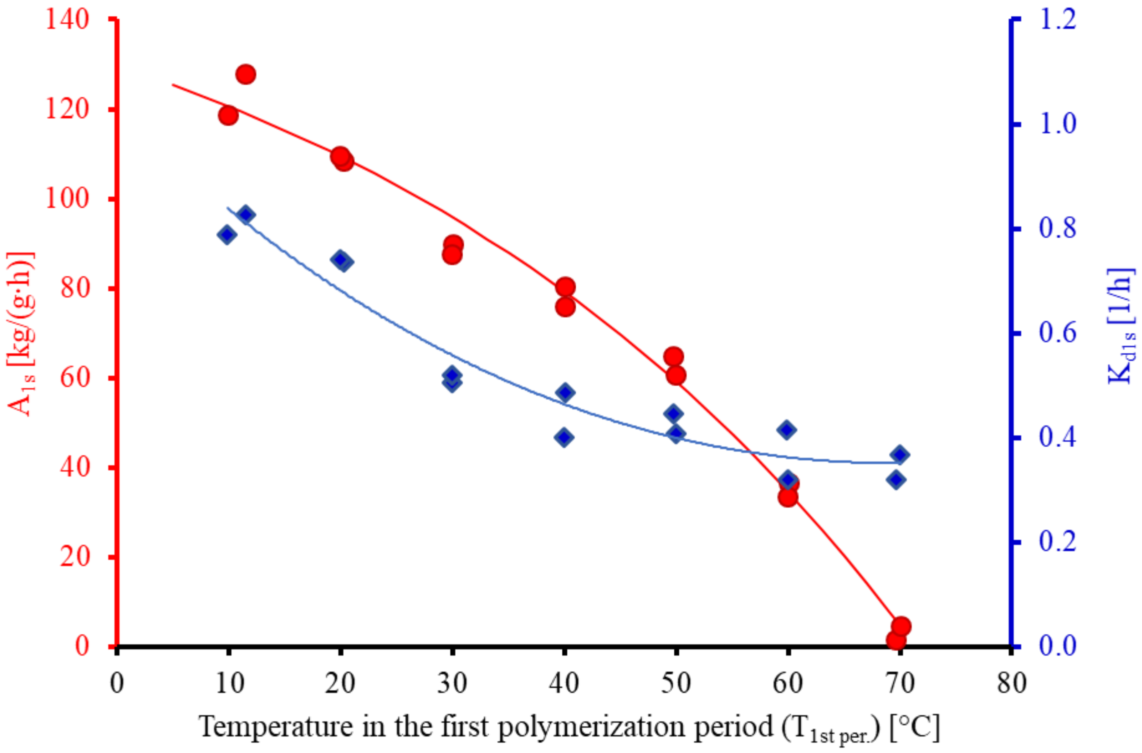

Figure 14: Correlation of optimized parameters for the second order of deceleration, ●A_{1s}, ♦K_{d1s}; m_{cat} = 4 mg, TEA/Ti = 120 mol/mol, n_{H2} = 32 mmol.

While the three parameters optimized for the first order of kinetic approach don't form any correlation, as presented in Figure 13, the two parameters of the second order approach (Figure 14) indicate a good ability to be fitted to some subsequent functional expressions, as they both follow smooth monotone trends.

One explanation for these results might be as follows: During the optimization process of the first order approach, the parameters A_{1f} and A_{2f} both related to the maximum polymerization rate at zero time partially compensate each other. This effect, however, also disturbs the single parameter K_{d1f}, which describes the deceleration features of the polymerization rate.

Moreover, the parameter A_{2f}, here representing stationary active centers in the first order approach, is naturally regarded as unrealistic. Thus, the second order kinetic approach is the most appropriate for a mathematical description of the observed kinetic curves. However, further research will be necessary to elucidate an explanation for the chemistry behind this finding.

6.2 3-PART CASCADE POLYMERIZATION

6.2.1 Activation Zone of 3-Part Cascade Reactor

The activation zone of the 3-part cascade reactor is the section where the catalyst suspension was mixed with propene and TEA. Two different mixing approaches were chosen for the study. In the first type of activation zone, the TEA solution is fed from four sides perpendicular to the flow of catalyst suspension (Figure 15, left).

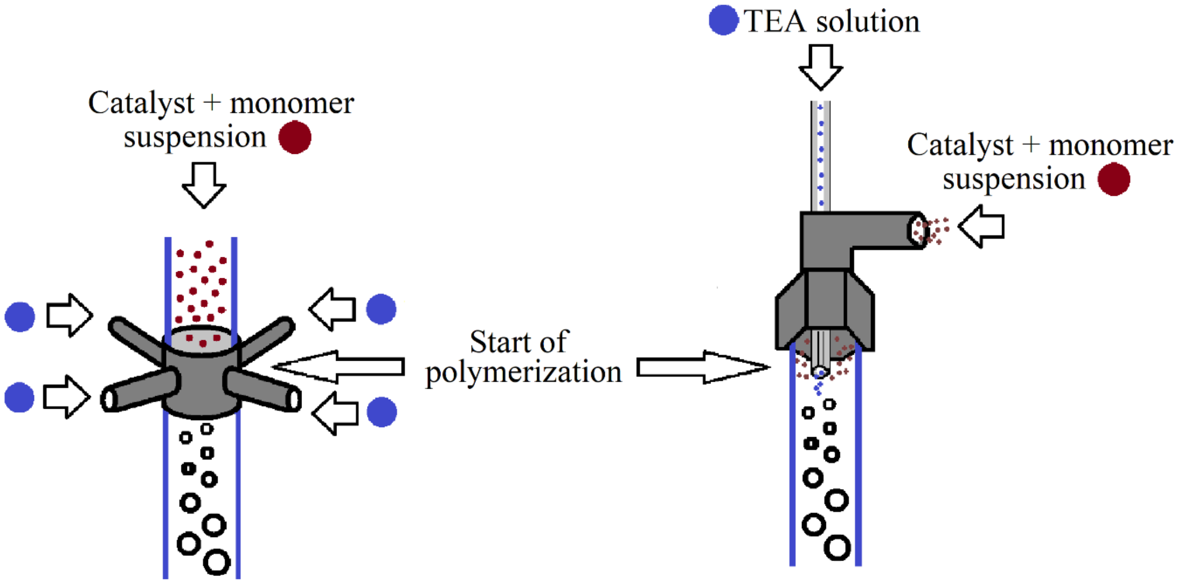

Figure 15: Two different mixing approaches of catalyst suspension with TEA. TEA supply by 4-side injection (left); TEA supply by needle (right).

The perpendicular mixing of the streams results in immediate homogenization of catalyst and cocatalyst. The position where the catalyst suspension stream and the TEA solution are mixed is defined as the polymerization start point. However, during polymerization with this set-up (Figure 15, left), the catalyst powder sticking to the metal parts of the cocatalyst junction inlet was observed, resulted in undefined polymer particles grow at this point. In the case of this activation system, small amounts of polymer were found at the inlet of the TEA solution after polymerization. This sticking effect of the catalyst causes an inhomogeneous flow of catalytic particles, resulting in higher productivity (10.2 vs 2.13 kg_{PP}/mol_{Ti}), molar mass (M_{n} = 52 vs 102 kg/mol) and polydispersity (3.8 vs 5.2) compared to the second type of activation zone, based on the needle (Figure 15, right). This capillary is introduced into the middle of the catalyst suspension stream and instant homogenization is achieved by turbulent flow.

Figure 16 shows GPC curves of polymers synthesised with different types of activation zones. The broader peak in a case with 4-side TEA injection confirms the inhomogeneous residence time of catalytic particles. For this reason, the needle type of activation zone was used in all the experiments carried out in this thesis.

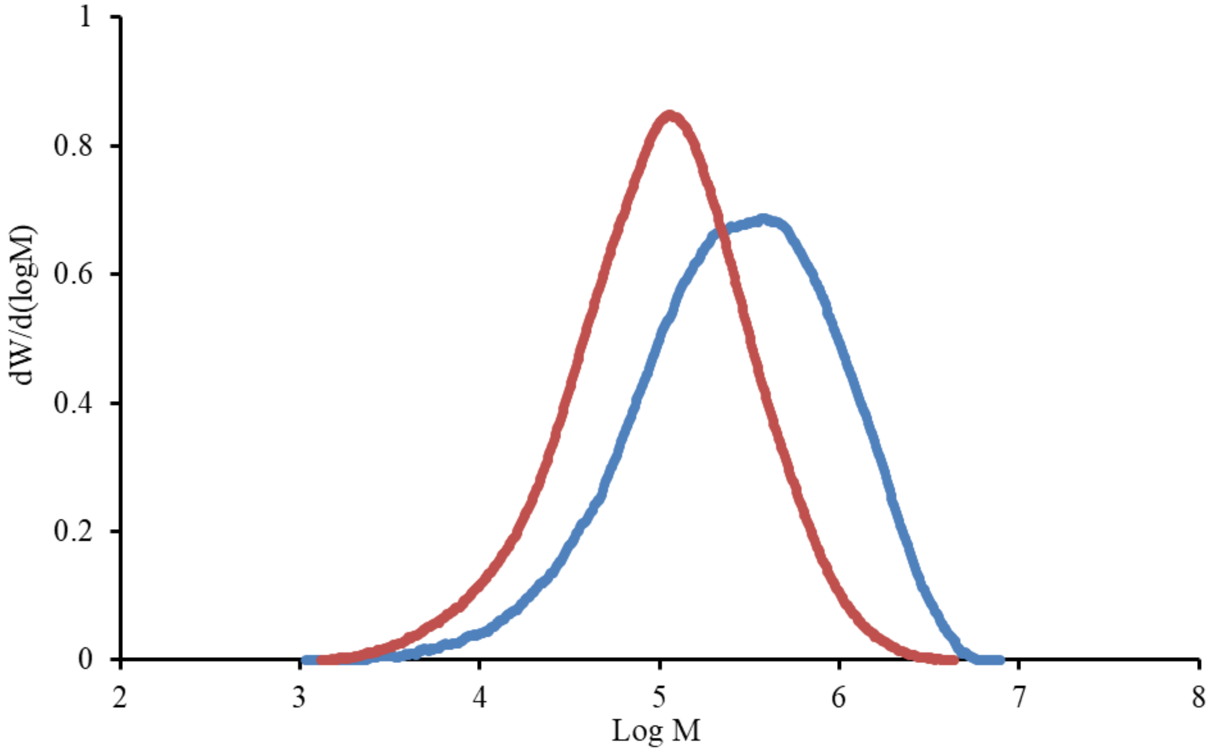

Figure 16: GPC curves of polymers synthesised with different types of activation zones. ● *4-sided TEA inlet,* ● *Needle system, Termination system CO in propene;* $T_{pol.}$ *= 40 °C; p = 2.1 MPa; TEA/Ti = 2000 mol/mol; CO termination concentration 0.21 mol. %.*

6.2.2 Termination Zone of 3-Part Cascade Reactor

The thesis focuses on the application of the stopped-flow apparatus to the method of prepolymerization under industrial conditions, rather than on basic research in the field of stopped-flow polymerization. Thus, the stopped-flow apparatus was modified for reversible termination of polymerization reaction. The purpose of the research was to subsequently reactivate the stopped-flow prepolymerized catalyst in the 4-litre batch reactor.

In the second part of the cascade reactor, stream of liquid monomer, catalyst and TEA was mixed with terminating agent. The efficiency of the termination is characterised by the polymerization activity (or the productivity g_{PP}/mol_{Ti} ratio), the molar mass and polydispersity of the synthesised polymer. The titanium concentration corresponds to the amount of catalyst.

Two types of terminating agent dissolved in liquid propene were used in this research. First, carbon monoxide as a non-reversible terminating system and second, carbon dioxide, as reversible terminating system. Both systems interact directly with active center of catalyst. The aim of the termination system was to terminate all active centres as quickly as possible. If the concentration of the terminating agent is sufficient, the polymerization activity remains constant even with increasing catalyst concentration in the capillary reactor. For this reason, the dependence of the productivity [g_{PP}/mol_{Ti}] on the concentration of the flowing titanium in the propene stream was measured with constant terminating agent flow.

6.2.2.1 Termination System Based on Carbon Dioxide/Propene

Carbon dioxide in liquid propene was suggested as the second termination system. The active center terminated by a CO_2 molecule can be reactivated by the addition of TEA.

The saturation of CO_2 in liquid propene was carried at 46 °C up to a pressure of 2.1 MPa, (concentration of 0.91 mol. %). The productivity of the synthesised polymers and their M_n are shown in Figure 17. Despite the low dependence of M_n on titanium concentration, a strong dependence of productivity on titanium concentration is evident.

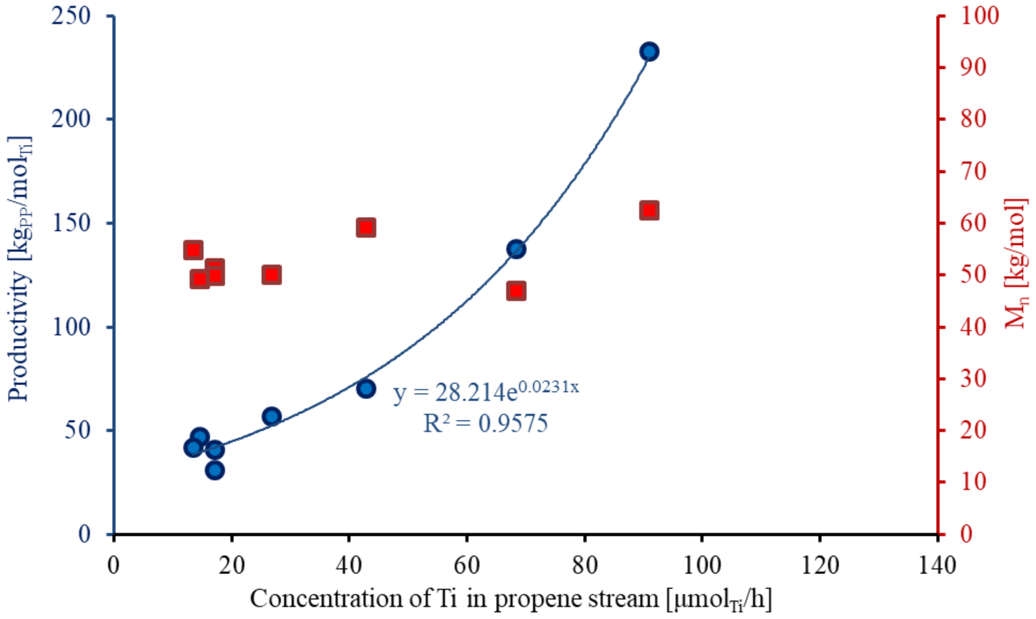

Figure 17: Dependence of polymer productivity and molar mass on concentration of titanium in monomer stream. Termination system CO_2 in propene, $T_{pol.}$ = 40 °C; p = 2.1 MPa; TEA/Ti = 2000 mol/mol; CO_2 termination concentration in propene 0.91 mol. %.

6.2.2.2 Influence of Termination System Concentration

A further optimization of the termination was to increase the CO_2 concentration in the liquid propene. The temperature of the 8-litre reactor was lowered, resulting in a reduction in the saturated vapour pressure of propene. After reducing the pressure of termination system, next CO_2 was added to the same pressure level. Figure 18 shows dependence of productivity and M_n of synthesised polymers on the concentration of CO_2 in the reaction system of propene stream in needle glass reactor. The molar flow rate of Ti in propene stream of evaluated polymers was 27 μmol_{Ti}/h. Based on the dependence, it was found that the concentration of terminating agent significantly affects both of these properties.

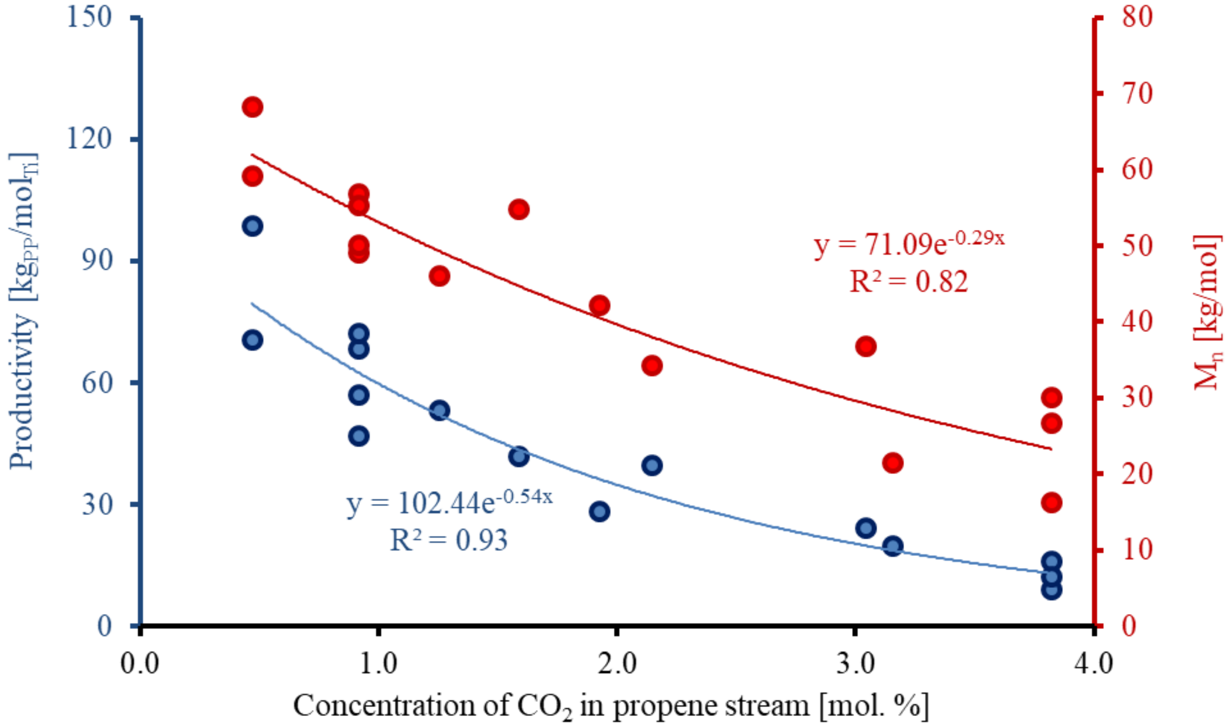

Figure 18: Dependence productivity and number-average molar mass of polymers on the concentration of the CO_2 termination system in propene stream; $T_{pol.}$ = 40 °C; p = 2.1MPa; TEA/Ti = 2000 mol/mol, cat. flow = 27 μmol_{Ti}/h.

6.2.3 Influence of Stopped-Flow 3-Part Reactor on Catalyst Performance

Ziegler-Natta catalysts are substances that are sensitive to impurities. Their activity rapidly decreases in the presence of polar compounds as water or oxygen. This fact is one of the most important issues in prepolymerization in SF apparatus. For this reason, the purity of the stopped-flow apparatus was evaluated before starting the reactivation experiments. Catalyst was subjected to process simulating polymerization in 3-part cascade reactor in the stopped-flow apparatus, but without the addition of TEA cocatalyst. After this blank experiment, the catalyst was isolated, transferred to mineral oil and tested in 4-litre batch reactor under the conditions of the 2nd polymerization period. Then the purity of the SF system was evaluated by comparing the activity of original catalyst and the catalyst exposed to the SF apparatus. By comparing the particle size distributions (PSD) (Figure 19), it was found out that exposure to the stopped-flow apparatus did not cause fragmentation of the catalyst.

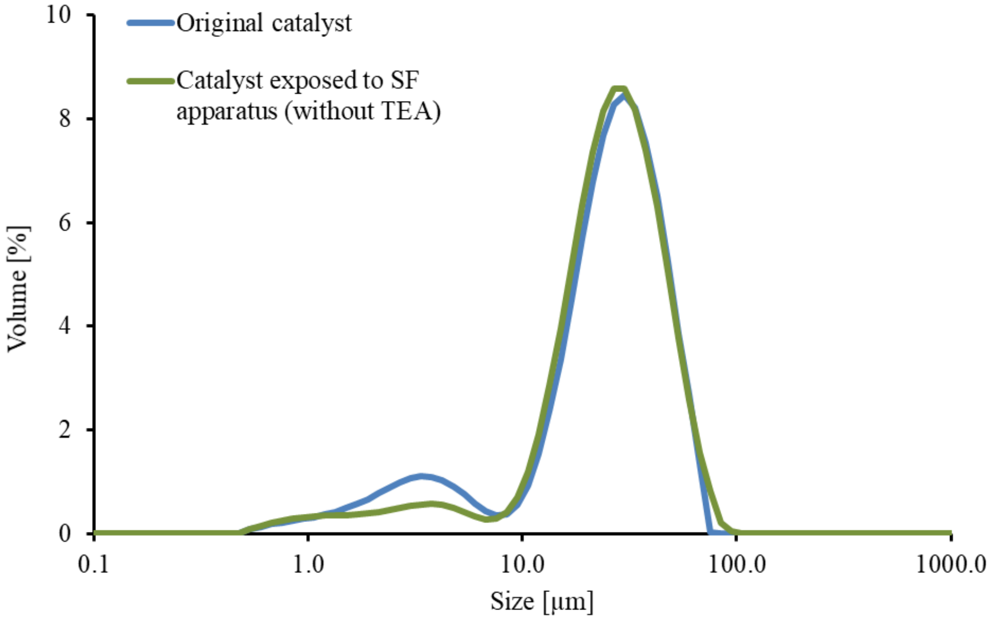

Figure 19: PSD of original catalyst and catalyst after exposure to SF apparatus (without TEA).

After catalyst exposure in the stopped-flow apparatus, polymerization was carried out in batch reactor. Polymerization conditions were identical to those of the 2nd polymerization period starting at 40 °C. Figure 20 shows kinetic profiles of batch polymerization with original catalyst (green) and polymerization with catalyst exposed to the SF apparatus (brown). The comparison of the curves shows that SF apparatus did not change shape the kinetic curve of the catalyst.

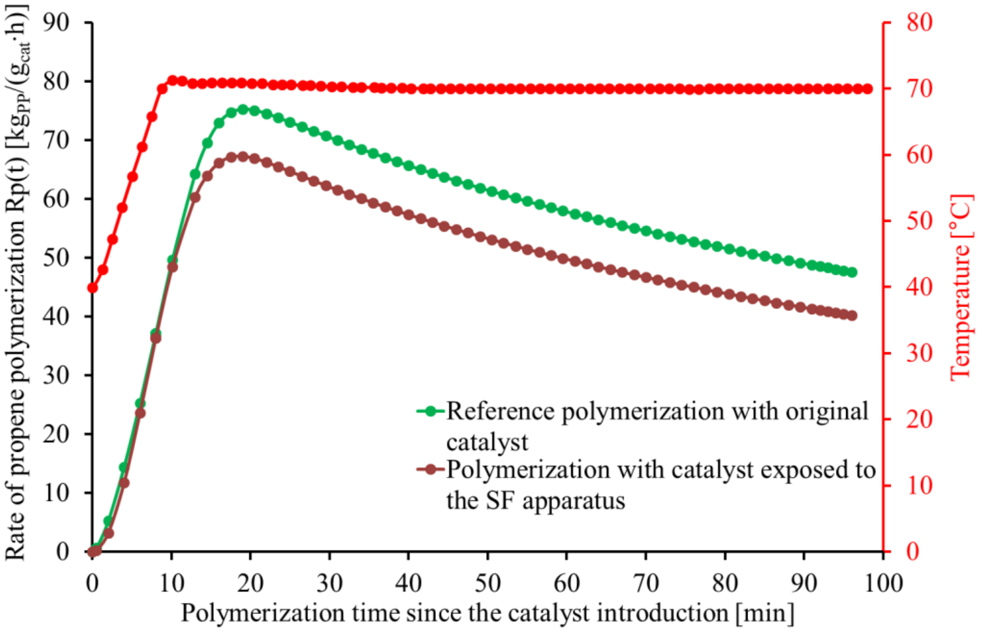

Figure 20: Kinetic profiles of bulk polymerization; m_{cat} = 4 mg; ● Reference polymerization; ● Polymerization with catalyst exposed to the SF apparatus.

These results confirmed that the stopped-flow apparatus with 3-part cascade system and the method of catalyst isolation are applicable for the project focused on the catalyst prepolymerization in SF apparatus as the 1st period of two-period polymerization experiment.

6.3 CATALYST PREPOLYMERIZATION BY USING 3-PART CASCADE REACTOR

6.3.1 PSD of Catalysts after 1st period of polymerization

The catalysts polymerized by different 1st period methods and at different temperatures were evaluated by particle size distribution method. The data in Figure 21 confirm the expected trend that particle size increases with increasing temperature in addition to increasing yield. Furthermore, it can be seen that both of 1st period polymerization methods did not caused the fragmentation of catalytic particles.

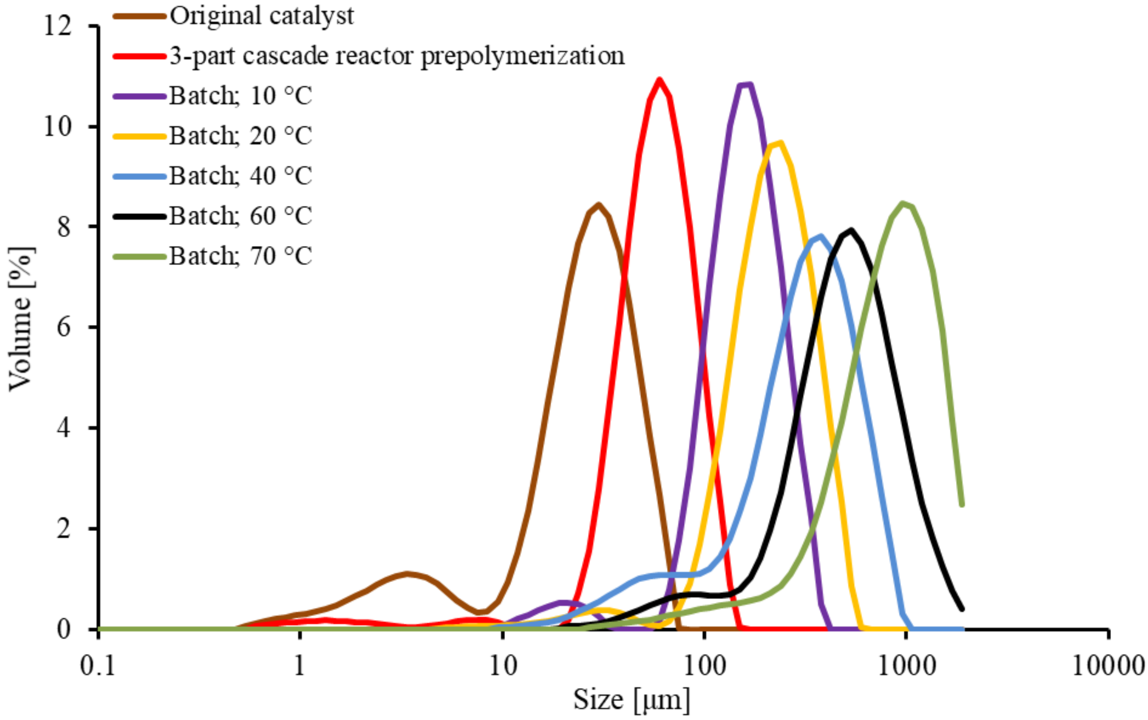

Figure 21: PSD of original non-prepolymerized catalyst and catalysts after different 1st method polymerization.

6.3.2 Effect of Prepolymerization in 3-Part Cascade Reactor

Figure 22 shows the difference in the kinetic profiles between the batch polymerization with non-prepolymerized catalyst exposed to the 3-part cascade reactor in SF apparatus and batch polymerization with catalyst, which was prepolymerized in 3-part cascade reactor at reversibly terminated by CO_2. The maximum polymerization rate was reached in both cases around 17 min after catalyst injection into 4-litre reactor. It can be seen that few minutes after the temperature reaches 70 °C, the rate of polymerization decreases in the case of polymerization with non-prepolymerized catalyst. This trend did not occurred in the case of polymerization with prepolymerized catalyst, where the kinetic profile shows a very stationary pattern. However, polymerization with non-prepolymerized catalyst is characterised by a higher rate of polymerization.

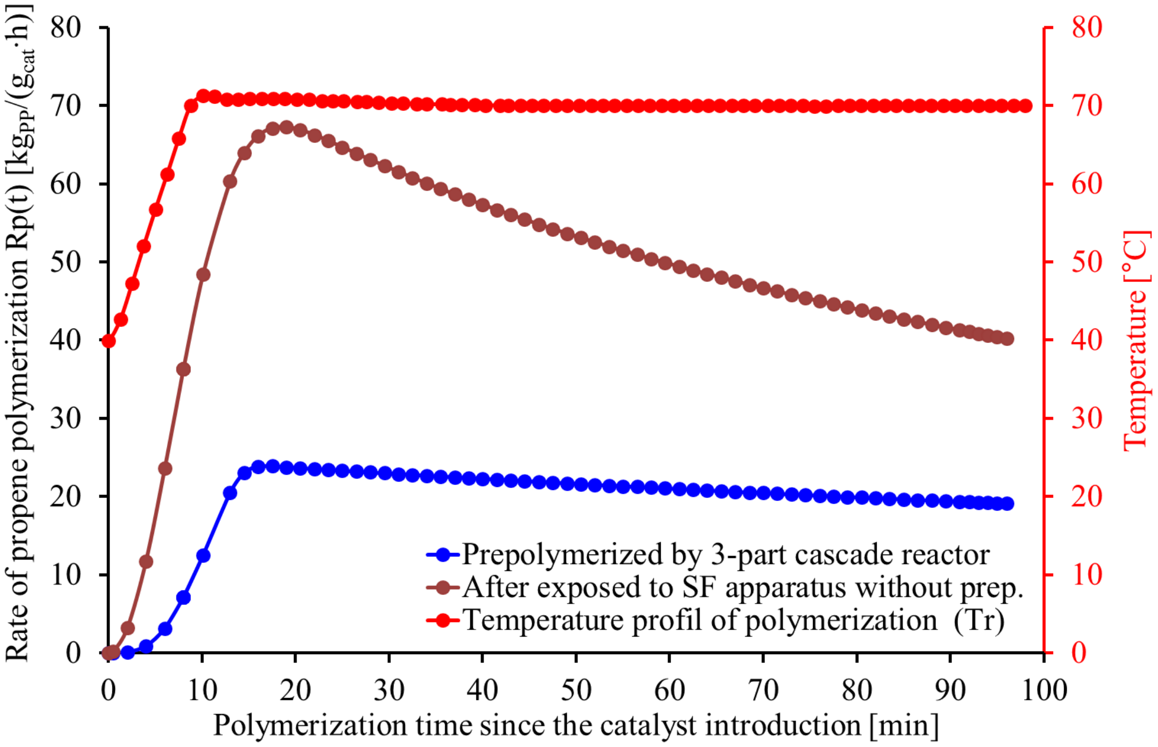

Figure 22: Kinetic profiles of bulk polymerization; ● Catalyst exposed to the 3-part cascade reactor without activation by TEA; ● Catalyst prepolymerized in 3-part cascade reactor (TEA/Ti ratio = 208 mol/mol, CO_2 termination concentration 3.82 mol. %, prepolymerization degree 15.6 g_{PP}/g_{cat}); ● Temperature profile of polymerizations.

6.3.3 Influence of TEA/Ti Ratio on Activity and Kinetic Profile

The catalyst reversible terminated in 3-part cascade reactor was reactivated by TEA. Reactivation of catalyst terminated by CO_2 was studied by polymerizations performed with different TEA/Ti molar ratios. The experiments were carried out at 70 °C for 90 min with TEA/Ti ratio 62, 104, 208 and 418 mol/mol.

Figure 23 shows kinetic profiles of batch polymerization experiments performed with SF prepolymerized and reversibly terminated catalyst. In all cases stationary behaviour without sharp decrease of polymerization rate after reaching 70 °C was observed. From the comparison of the curves it is clear that kinetic profiles of catalyst prepolymerized in SF apparatus are affected by TEA/Ti ratios lower than ca. 200 mol/mol.

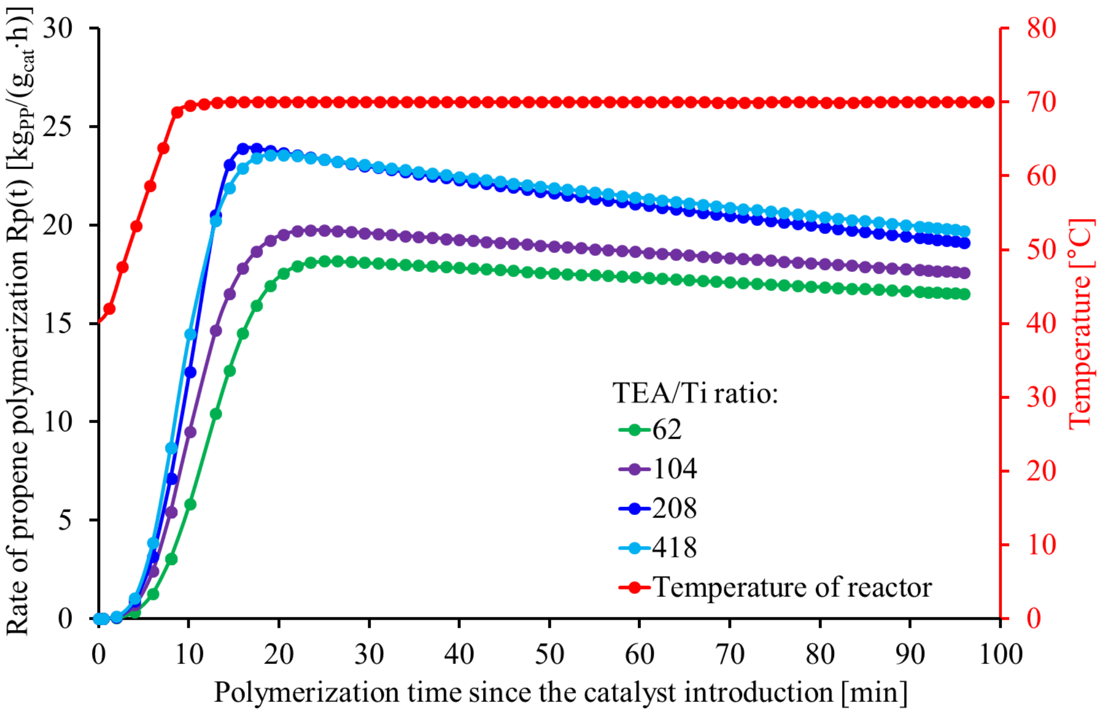

Figure 23: Kinetic profiles of polymerizations with different TEA/Ti molar ratios (2^{nd} order model); SF prepolymerized catalyst, CO_2 termination concentration 3.82 mol. %, prepolymerization degree 15.6 g_{PP}/g_{cat}, m_{cat} = 8.6 mg, n_{H2} = 32 mmol.

7 CONCLUSION

Thesis is focused on the kinetic profiles of two-period propene polymerizations with diether based Ziegler-Natta $MgCl_2$-supported catalyst. The influence of the 1st polymerization period, on the kinetic profile of the 2nd period carried out at 70 °C for 90 min in liquid propene in a stainless steel batch reactor, was determined. It was found that both of the 1st period methods (stopped-flow and batch prepolymerization) used in the research significantly affect kinetic profiles of the 2nd polymerization period.

Subsequently, a procedure was developed to evaluate the kinetics of the 2nd period of propene polymerization. Experimental points of kinetic profiles were utilized as input data for kinetic models of active centers deactivation according to the first and second order. For better resolution, the deceleration part of the kinetic functions was evaluated by difference between the temperature of the reactor and the temperature of the incoming water (DT). The model was fitted based on a simplex optimization procedure that fits the experimental data with high accuracy using semi-empirical equations. The deviations of both models are similar for each polymerization experiments, confirming their suitability.

In the case of the 1st method of the 1st period, carried out in batch reactor at seven different temperature levels in the range 10–70 °C in 350 ml of liquid propene, it was found that higher temperature of the 1st period leads to higher yield of the 1st period, lower yield of the 2nd period and more stationary kinetic profile. These results are confirmed by the decreasing dependence of the kinetic constants of the model, which is based on the deactivation of active centers according to the second order.

Despite the accurate fitting of the experimental data, the dependence of the kinetic constants on the temperature of the 1st period was only found for the second order model. The dependence of the kinetic constants on the prepolymerization temperature was not observed for the first order model. 1st period temperature does not affect melt flow rates and the xylene solubles of the resulting polymers.

In the case of prepolymerization temperature levels 20 and 40 °C, in addition to 120 mol/mol TEA/Ti ratio, the influence of 60 and 240 mol/mol TEA/Ti ratio on the kinetic profiles and properties of the polymers was described. For both temperature levels it was found that the total yield increased with increasing TEA/Ti ratio. This effect was more significant in the case of prepolymerization at 20 °C and is probably related to the monomer-dimer equilibrium of TEA. The dissociation of TEA is temperature dependent and at lower temperatures TEA is present in an inactive dimeric form. The relatively slow temperature ramp between polymerization periods slows the dissociation of TEA into its active form, resulting in slower activation of the catalytic particle. The slowing down of this exothermic reaction results in a slower release of heat from the catalytic particle into the surrounding space. Due to sufficiently fast heat transfer to the surroundings, the deactivation of the active centres of the catalyst due to local overheating is suppressed. This phenomenon is also related to the kinetic constants. The values of the kinetic constants A_{1s} and Kd_{1s} are higher in the case of a first period temperature level 20 °C, which corresponds to higher activity. Thus, the dissociation phenomenon is more significant at lower prepolymerization temperatures. The TEA/Ti ratio has no effect on the MFR and XS values.

The 2nd method of the 1st period was carried out by polymerization in stopped-flow apparatus in 3-part cascade polymerization reactor. For this reason, a procedure was developed for suitable reversible termination and isolation of the prepolymerized catalyst. The needle activation zone was found to sufficiently mix the TEA, catalyst and monomer without the accumulation of polymer powder in 3-part cascade polymerization reactor. Polymers prepared with this activation zone had lower M_n, M_w and polydispersity Đ than polymers prepared with four-sided activation zone.

The non-reversible terminating agent CO/propene was selected as the first termination system. With this termination system, a productivity of 1.25 kg_{PP}/mol_{Ti} was achieved at the most efficient termination. Using a CO_2/propene reversible termination system, a productivity of 233 kg_{PP}/mol_{Ti} with $M_w = 249$ kg/mol was achieved. The order of magnitude higher productivity is due to slower termination by the CO_2/propene mixture. Subsequent optimization of the reaction conditions by increasing the concentration of the terminating agent resulted in a more efficient termination with final productivity of polymerization 9.1 kg/mol, $M_w = 68$ kg/mol and $Đ \approx 4$. These conditions were used for the preparation of the catalyst prepolymerized in a 3-part cascade reactor in SF apparatus, which was subsequently used for the 2nd polymerization period. To confirm the suitability of the apparatus designed for 2nd method of prepolymerization, the catalyst was exposed to the 3-part cascade reactor in the Stopped-Flow apparatus without activation with TEA, subsequently isolated and its activity in bulk polymerization was compared with the reference polymerization. The activity of the catalyst, which was exposed to the SF apparatus without TEA addition, was determined to be 90 %.

Particle Size Distribution (PSD) of the original catalyst and the catalysts prepolymerized by both methods were compared. The catalyst with the lowest degree of prepolymerization, around 14.6 g_{PP}/g_{cat}, was prepared by prepolymerization in a 3-part cascade polymerization reactor in the SF apparatus. The degree of prepolymerization of catalyst prepared by the first prepolymerization method in the batch reactor was ranged from 74 to 11 000 g_{PP}/g_{cat} and depended on the polymerization temperature. Based on comparison of PSD curves of original and prepolymerized catalysts, no fragmentation was observed.

The activity of the 2nd polymerization period in the case of catalyst prepolymerized in the 3-part cascade reactor was lower than in the case of bulk prepolymerization, specifically 21.1 $kg_{PP}/(g_{cat} \cdot h)$ compared to ≈ 60 $kg_{PP}/(g_{cat} \cdot h)$. This may be due to insufficient reactivation of all active centers terminated by CO_2. However, the kinetic profile of polymerizations with a prepolymerized catalyst, which was reversibly terminated by CO_2, was significantly modified. After reaching the polymerization temperature, no immediate and significant decrease in polymerization activity was observed. The resulting kinetic profile showed a stationary behaviour with only a slightly decreasing trend. These observations are also described by the values of the kinetic constants K_{d1s}, which characterise the non-stationary behaviour of the polymerization system. The values of the K_{d1s} kinetic constants are significantly lower than in the case of polymerizations with the catalyst prepolymerized upon various temperatures employing the 1st method.

The optimum TEA/Ti ratio for reactivation of the reversibly terminated catalyst in the batch reactor was found to be around 200 mol/mol. At a lower ratio, the kinetic profile and kinetic constants are affected, the activity is lower and therefore full reactivation does not occur. The TEA/Ti ratio does not affect values of MFR and XS.

The ageing effect on the catalyst prepolymerized in 3-part cascade reactor was also studied. It was found that the activity of the catalyst decreased with time, especially within first 6 days after catalyst prepolymerization. Catalyst ageing affects activity but has no effect on the values of MFR and XS.

8 REFERENCES

1. Queiroz, A., Pedroso, G. B., Kuriyama, S. N., Fidalgo-Neto, A. A. (2020). Subcritical and supercritical water for chemical recycling of plastic waste. Current Opinion in Green and Sustainable Chemistry, 25, 100364. https://doi.org/10.1016/j.cogsc.2020.100364
2. Moore, E. P. (Ed.). (1996). *Polypropylene handbook: Polymerization, characterization, properties, processing, applications*. Hanser Publishers. ISBN: 978-1569902080
3. Soares, J. B. P., McKenna, T. F. L. (2012). *Polyolefin reaction engineering*. Wiley-VCH. ISBN: 9783527317103
4. Pasquini, N., Addeo, A. (Eds.). (2005). *Polypropylene handbook* (2nd ed). Hanser. ISBN: 978-1569903858
5. Kissin, Yu. V., Mezhikovsky, S. M., Chirkov, N. M. (1970). The stereospecific mechanism of olefin polymerization by heterogeneous complex catalysts—I. The degree of the catalyst surface filling with active sites and the chemical structure of the sites. *European Polymer Journal*, *6*(2), 267–279. https://doi.org/10.1016/0014-3057(70)90160-6
6. Severn, J., Jones, R. L. (2018). Stereospecific α-Olefin Polymerization with Heterogeneous Catalysts. In R. Hoff (Ed.), *Handbook of Transition Metal Polymerization Catalysts* (pp. 229–312). John Wiley & Sons, Inc. https://doi.org/10.1002/9781119242277.ch9
7. Chadwick J., Morini G., Balbontin G., Camurati I., Heere J. R., Mingozzi I., Testoni F. Effects of Internal and External Donors on the Regio- and Stereoselectivity of Active Species in $MgCl_2$-Supported Catalysts for Propene Polymerization. *Macromolecular Chemistry and Physics*, *1995–2002*(202). https://doi.org/10.1002/1521-3935(20010601)202:10<1995::AID-MACP1995>3.0.CO;2-L
8. Fallah, M., Bahri-Laleh, N., Didehban, K., Poater, A. (2020). Interaction of common cocatalysts in Ziegler–Natta-catalyzed olefin polymerization. *Applied Organometallic Chemistry*, *34*(2). https://doi.org/10.1002/aoc.5333
9. Ystenes, M. (1991). The trigger mechanism for polymerization of alpha-olefins with Ziegler-Natta catalysts: A new model based on interaction of two monomers at the transition state and monomer activation of the catalytic centers. *Journal of Catalysis*, *129*(2), 383–401. https://doi.org/10.1016/0021-9517(91)90043-4
10. Terano, M., Kataoka, T. (1989). A kinetic study of propene polymerization using $MgCl_2$-supported catalysts. *Die Makromolekulare Chemie, Rapid Communications*, *10*(2), 97–102. https://doi.org/10.1002/marc.1989.030100210
11. Zhang, Z., Jiang, B., He, F., Fu, Z., Xu, J., Fan, Z. (2019). Comparative Study on Kinetics of Ethylene and Propylene Polymerizations with Supported Ziegler–Natta Catalyst: Catalyst Fragmentation Promoted by Polymer Crystalline Lamellae. *Polymers*, *11*(2), 358. https://doi.org/10.3390/polym11020358
12. Kissin, Y. V. (2003). Multicenter nature of titanium-based Ziegler-Natta catalysts: Comparison of ethylene and propylene polymerization reactions. *Journal of Polymer Science Part A: Polymer Chemistry*, *41*(12), 1745–1758. https://doi.org/10.1002/pola.10714
13. Liu, B. Matsuoka, H. Terano, M. (2001). Stopped-Flow Techniques in Ziegler Catalysis. *Macromol. Rapid Commun*, *2001*(22), 1–24. https://doi.org/10.1002/1521-3927(20010101)22:1<1::AID-MARC1>3.0.CO;2-T
14. Hoza, A. (2017). *Effect of Ethylene and Propylene on Performance of Ziegler – Natta Catalyst in Stopped – Flow Polymerization.* [PhD Thesis] Brno University of Technology, Faculty of Chemistry

ABSTRACT

Thesis is focused on the kinetic profiles of two-period polymerizations of propene with diether based Ziegler-Natta $MgCl_2$ supported catalyst. The effect of two methods characterising the 1st polymerization period, on the kinetic profile of the main the 2nd period carried out at 70 °C for 90 min in a stainless steel batch reactor, was described. The kinetic profiles based on the heat transfer data of the 2nd periods were fitted and characterised by two models.

The 1st period was performed by two different methods with conditions similar to the industrial process. The 1st method was performed as 10 min polymerization in a batch reactor at seven temperature levels in the range 10–70 °C in 350 ml of liquid propene. In addition, at the 20 and 40 °C temperature levels, the effect of the cocatalyst per titanium ratio was also described. For the 2nd method, a stopped-flow (SF) apparatus with a 3-part cascade reactor was utilized. The polymer prepared by this method was reversibly terminated with carbon dioxide and subsequently reactivated during the 2nd polymerization period. For this method, the thesis also describes the types of activation zones, the influence of termination reagents concentration and the procedure for reversible termination of the catalyst.

The kinetic profiles of the 2nd polymerization period were fitted by simplex optimization procedure by suitable semi-empirical equations. These were derived from fundamental kinetic approaches using the first and the second order of the catalyst active centers decay. The kinetic constants of these models describe the behaviour of the system with the prepolymerized catalyst during the 2nd polymerization period. Based on the correlation between the 1st polymerization period conditions and the kinetic constants, the differences and the suitability of the models for further mathematical operations were discussed.

The synthesised prepolymerized catalysts and the resulting polymers were analysed and characterised by structural analytical methods. The resulting properties such as molar mass, polydispersity, melt flow rate, xylene solubles and particle size distribution were evaluated.